

1-1-2022

Effect of biochar on desiccation of marine soils under constant and cyclic temperatures

Thellen Kumar Puspanathan

Vihan Shenal Jayawardane

Suvash Chandra Paul

Kong Sih Ying

Sanjay Kumar Shukla

Edith Cowan University, s.shukla@ecu.edu.au

See next page for additional authors

Follow this and additional works at: <https://ro.ecu.edu.au/ecuworks2022-2026>



Part of the [Geotechnical Engineering Commons](#)

10.1007/s11440-022-01613-6

Puspanathan, T. K., Jayawardane, V. S., Paul, S. C., Ying, K. S., Shukla, S. K., & Anggraini, V. (2022). Effect of biochar on desiccation of marine soils under constant and cyclic temperatures. *Acta Geotechnica*, 1-24. Advance online publication. <https://doi.org/10.1007/s11440-022-01613-6>

This Journal Article is posted at Research Online.

<https://ro.ecu.edu.au/ecuworks2022-2026/933>

Authors

Thellen Kumar Puspanathan, Vihan Shenal Jayawardane, Suvash Chandra Paul, Kong Sih Ying, Sanjay Kumar Shukla, and Vivi Anggraini



Effect of biochar on desiccation of marine soils under constant and cyclic temperatures

Thellen Kumar Puspanathan¹ · Vihan Shenal Jayawardane¹ · Suvash Chandra Paul² · Kong Sih Ying¹ · Sanjay Kumar Shukla³ · Vivi Anggraini¹

Received: 8 August 2021 / Accepted: 6 June 2022
© The Author(s) 2022

Abstract

Biochar has recently been gaining increasing attention as a stable and sustainable soil amendment material. However, the effect of biochar amendment on the desiccation behaviour of coastal soils has not yet been examined. Consequently, the present study primarily investigated the effect of exposing biochar-amended marine soil (BAS) to constant and cyclic temperatures on its swell–shrink, evaporation and desiccation cracking characteristics. Biochar contents of 1%, 2%, 4% and particle size ranges of PS-1 ($600 \mu\text{m} < D \leq 2000 \mu\text{m}$), PS-2 ($300 \mu\text{m} < D \leq 600 \mu\text{m}$), PS-3 ($D \leq 75 \mu\text{m}$) (D : biochar particle diameter) were employed. It was revealed that the absolute volumetric shrinkage of both unamended and biochar-amended specimens increased as the number of thermal cycles increased. Under continuous heat exposure, 4% (PS-3) BAS in compacted state achieved the maximum reduction in volumetric shrinkage which was 42%. Moreover, under continuous heat exposure, 2% (PS-1) BAS in slurry state achieved the highest reduction in desiccation cracking, which was 73%. The present study highlights the importance of identifying the most effective combination of biochar content and particle size required to achieve a desired outcome, in order to gain the maximum benefit of biochar as an amendment material at the lowest possible cost.

Keywords Biochar · Cracking · Desiccation · Evaporation rate · Marine soil · Shrinkage

✉ Vivi Anggraini
vivi.anggraini@monash.edu

Thellen Kumar Puspanathan
tkkp1@student.monash.edu

Vihan Shenal Jayawardane
vihan.jayawardane@monash.edu

Suvash Chandra Paul
suvashpl@iubat.edu

Kong Sih Ying
kong.sih.ying@monash.edu

Sanjay Kumar Shukla
s.shukla@ecu.edu.au

¹ Civil Engineering Discipline, School of Engineering, Monash. University Malaysia, Jalan Lagoon Selatan, 47500 Bandar Sunway, Selangor Darul Ehsan, Malaysia

² Department of Civil Engineering, International University of Business Agriculture and Technology, Dhaka 1230, Bangladesh

³ School of Engineering, Edith Cowan University, 270 Joondalup Drive, Joondalup, Perth, WA 6027, Australia

1 Introduction

The rapid growth of economic and social development in recent years has led to an increase in demand for usable land, forcing the developers to maximize the usage of any available land. Coastal areas have now become popular sites for land development despite the poor engineering properties of marine soil that primarily makes up the sub-grade in coastal regions [14]. Marine soil is generally composed of minerals that possess swelling properties, hence causing the soil to have low strength and stability [8]. Additionally, studies have reported soil desiccation serving as a reason for settlements of structures [35, 56]. Desiccation is a common issue among plastic soils which involves the loss of moisture when subjected to heat. The gradual reduction in water content within soil pores results in an increased soil suction [53]. As moisture leaves, voids are created within the soil particles. With further reduction of moisture, the water pressure within the soil is greatly reduced, as a result there is an increase in effective stresses

which induces the soil matrix to undergo internal compression [44]. Hence, the soil is seen to experience a reduction in volume, recognized as shrinkage [50].

Shrinkage results in soil volume changes and may induce crack formation as well [47]. Shrinkage of soil can be associated with several reasons, primarily the initial moisture content and also the extent to which the soil is exposed to desiccating conditions [46]. Soil in field conditions may often be exposed to wet–dry and/or thermal cycles throughout the year [4]. In such situations, soil is highly subjected to cracking as it desiccates. Al Zubaydi and Lecture [2] reported that clayey soils collected from the city of Mosul experienced increased volumetric reduction with every subsequent wetting–drying cycle up to four cycles. Similar results were reported by Albrecht and Benson [3] where clayey soils which were subjected to wetting–drying cycles experienced irreversible shrinkage. When soils were exposed to wetting conditions after experiencing drying, it was expected that the soil would swell to its original state. However, instead, the soil was noticed to experience reduced swelling. According to Basma et al. [7], during cyclic wetting and drying soil may experience either partial or full shrinkage. If the soil experiences partial shrinkage, the voids will be reduced preventing the soils from completely taking up water during the subsequent wetting phase and in turn allowing it to receive water and inhabit it from completely swelling only partially. In another study conducted by Sridharan and Allam [51], it was reported that the constant wetting and drying lead to aggregation of clay particles which resulted in the generation of bigger inter-pores. In the meantime, continuous wetting and drying of weakly bonded clay soils could lead to reduction in its swell capability due to destruction to the bonds between the clay minerals and change in the soil structure.

In an effort to reduce the occurrence of desiccation cracks in soils, in recent years there has been a great interest towards the incorporation of biochar into soils [65]. Biochar is a material generated through the thermal degradation of organic materials without the presence of air (i.e. oxygen) also known as pyrolysis [26]. It is found to alter the porosity of soils [9]. In coarse-grained soils, biochar could increase the water holding capacity and enhance the stability of soil aggregates, thus changing the evaporation properties of the soil [18]. However, adding large amounts of biochar would increase the porosity of the soil due to an increase in micropores [4]. In a study by Yang et al. [60] biochar was used as a medium to reduce water loss and desiccation cracks. Evaluating the effect of different biochar percentages on the soil water evaporation, reported that the addition of biochar decreases the soil fractal dimension and increased the moisture content.

Thus far, to the authors' best knowledge, no work has been carried out to specifically scrutinize the effect of biochar incorporation on the desiccation behaviour of a coastal region soil (such as marine soil) subjected to cyclic and constant temperatures. Therefore, in the present study, biochar-amended marine soil has been exposed to both constant and cyclic temperatures and an in-depth analysis of the resulting variations in its swell–shrink characteristics, evaporation rate and desiccation cracking magnitude have been carried out.

2 Materials and methodology

2.1 Marine soil

The coastal region soil employed for the present study was marine soil, which was obtained from the vicinity of the coastal region of Pantai Remis located in Sg Sembilang, Jeram in the state of Selangor, Malaysia (3° 12' 17.5" N and 101° 18' 18.0" E). The basic geotechnical and thermal properties of marine soil are listed in Table 1. Based on the conducted sieve hydrometer and Atterberg limit tests, marine soil was classified as a “very clayey sand with

Table 1 Basic properties of marine soil

Property	Value
Natural moisture content (%)	143.44
Particle size distribution (%)	
Gravel	–
Sand	79
Silt	15.5
Clay	5.5
Fines content	21
Atterberg limits (%)	
Liquid limit	37
Plastic limit	23
Plasticity index	14
Compaction properties	
Maximum dry density (MDD) (g/cm ³)	1.22
Optimum moisture content (OMC) (%)	22.2
Specific gravity	2.44
Activity	2.59
BSCS	SCI
Thermal properties	
Thermal conductivity (W/m K)	1.346
Volumetric heat capacity (J/m ³ K)	2294
Thermal diffusivity (mm ² /s)	0.587
Thermal resistivity (°C cm/W)	74.3

intermediate plasticity (SCI)” in conformation with the British Soil Classification System for Engineering Purposes (BSCS). Numerous researchers in the past have mentioned that sandy/coarse textured soils are generally more responsive towards biochar amendment compared to clayey/fine textured soils, owing to the significant size difference that exists between the biochar particles incorporated and the coarse soil grains. In essence, the greater the clay content present within the soil that is amended, the lesser the influence exerted by biochar on the amended soil [9, 29, 57, 58]. Therefore, in the case of the present study, it was expected that biochar amendment would lead to notable alterations in the properties of marine soil tested, since it was determined to be primarily coarse textured in nature.

2.2 Palm Biochar

According to Blanco-Canqui [9], biochar produced at high temperatures (≥ 500 °C) are more likely to retain water and are less likely to resist water absorption. This is due to the removal of hydrophobic materials that exist on the surface of the biochar particles during pyrolysis at high temperatures. Therefore, “palm biochar”, which is known to originate from the thermal disintegration of palm biomass without the presence of oxygen, was employed as the biochar material for the present study, since it is produced at a high temperature of 500 °C. Accordingly, palm biochar was purchased from Eureka Synergy Sdn Bhd, Negeri Sembilan, Malaysia. The chemical composition and basic properties of palm biochar are listed in Table 2.

2.3 Material preparation & specimen notation scheme

Natural marine soil was found to have a natural moisture content of 143.44%, which made crushing unviable.

Table 2 Basic properties and chemical composition of Palm biochar

Property	Value
Total moisture (%)	< 10
Specific gravity	1.42
Chemical composition (%)	
Nitrogen	0.5–1.0
Phosphorous	0.3–0.5
Potassium	1.3–1.8
Total sulphur	0.1–0.2
Chlorine	0.3–0.4
Organic matter (%)	90–95
Pore size (Å)	20–22

Therefore, it was oven-dried for 3 days at 105 °C until a constant mass was achieved, crushed using a mechanical grinder into finer particles and then passed through a 2.36-mm sieve to ensure soil uniformity. For the present study both “content” and “particle size (PS)” of palm biochar were varied and their effects on marine soil were assessed. In order to make a decision on the appropriate biochar contents and particle sizes that would be employed for the amendment of marine soil, an extensive literature study was conducted that specifically focused on past works that utilized biochar as amendment material for soils. Consequently, the biochar amendment contents selected for the present study were based on studies conducted by Bordoloi et al. [10], Yang et al. [60], Zhang et al. [65], Zong et al. [67], the were 0%, 1%, 2% and 4%, respectively. Moreover, the biochar particle sizes selected for the present study were based on studies conducted by Hussain et al. [20], Villagra-Mendoza [57] and Wang et al. [59]. Accordingly, palm biochar was crushed using a mechanical grinder and sieved to obtain three specific particle size ranges (Fig. 1). The crushed marine soil passing 2.36 mm sieve was then mixed with the designated contents and particle size ranges of palm biochar (based on the different requisites of each experiment) by dry weight of the total mixture. Specimen notations that were employed for the present study, based on amendment content and amendment particle size, are listed in Tables 3 and 4, respectively.

2.4 Modified compaction tests

A series of compaction tests were conducted using the mini-compaction apparatus to determine the optimum moisture content (OMC) and maximum dry density (MDD) of the natural marine soil and PS-3 biochar-amended soil (BAS) specimens and [52]. The soil–biochar mixture was ensured to be evenly mixed, prior to adding the intended amount of distilled water. Upon adding distilled water, the mixture was mixed until a uniform consistency was achieved. The compaction procedure was then carried out immediately in order to prevent loss of moisture from the mixture. Subsequently, the MDD and OMC of the tested soil specimens were determined. The deduced MDD and OMC values for the corresponding soil mixtures were then used to prepare specimens for the thermal cycle and desiccation tests.

2.5 Thermal cycle experiments

During daytime, marine soil in the field would generally be exposed to a high temperature as a result of solar radiation and would consequently experience desiccation. Conversely, during night-time, the soil would be exposed to a much cooler temperature and would most likely experience

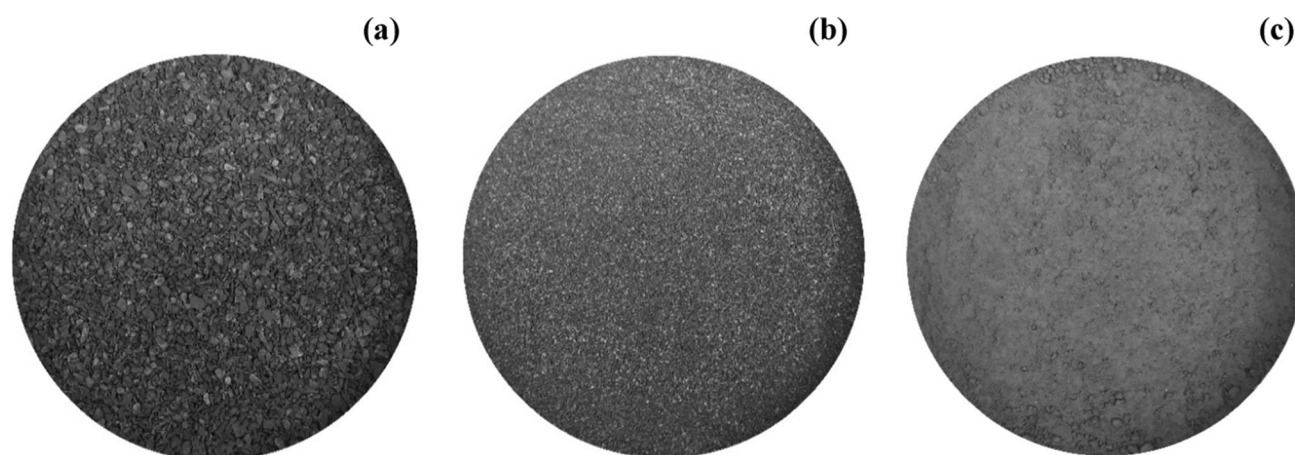


Fig. 1 Palm biochar particle size ranges: **a** PS-1; **b** PS-2; **c** PS-3

Table 3 Specimen notations based on amendment content

Notation	Description
NS	Natural marine soil
1% BAS	1% biochar amended soil
2% BAS	2% biochar amended soil
4% BAS	4% biochar amended soil

Table 4 Specimen notations based on amendment particle size

Notation	Description
PS-1	$600 \mu\text{m} < D \leq 2000 \mu\text{m}$
PS-2	$300 \mu\text{m} < D \leq 600 \mu\text{m}$
PS-3	$D \leq 75 \mu\text{m}$

wetting owing to the condensation of water vapour in the atmosphere [23, 45]. The daytime hours (drying of the soil) and night-time hours (cooling and wetting of the soil) that constitute the 24 h of a day is generally referred to as one thermal cycle (or diurnal cycle). On the field, continuous exposure of marine soil to recurrent daily thermal cycles leads to its repetitive drying, cooling and wetting which in turn, presumably leads to significant deformations. Therefore, to gauge the effect of biochar incorporation on the deformation behaviour of marine soil exposed to continuous thermal cycles, unamended and biochar-amended soil specimens were subjected to a series of thermal cycle experiments.

Specimens were prepared by compacting the unamended and PS-3 biochar-amended soil mixtures to their predetermined MDDs and OMCs and set up in oedometer cells. The specimens were left to soak and swell in the oedometer cells under an applied seating load of 6.25 kPa

for a duration of fifteen hours at room temperature to simulate overnight cooling and wetting experienced by the soil due to condensation of water vapour on the field [19, 23, 45]. During the wetting period, free swell values of the soil specimens were recorded at designated time intervals. Following the wetting phase, the specimens were removed from the oedometer cells and transferred to an oven where they were exposed to an elevated temperature of 60 °C for seven continuous hours [19]. A temperature of 60 °C was employed to replicate the temperature likely experienced by marine soil on the field when exposed to solar radiation during daytime [5, 19, 48, 55]. Following seven hours, the specimens were removed from the oven and their heights were measured. Subsequently, images of the top and bottom of the specimens were captured with a camera for the conduction of a shrinkage analysis later using ImageJ software. The specimens were then once again set up in oedometer cells and left to soak for fifteen hours and the procedure for the thermal cycles was thus repeated until a total of four thermal cycles were completed.

2.6 Constant desiccation experiments

It is deemed necessary that a constant desiccation test be carried out, so as to analyse the effect of biochar amendment on the shrinkage behaviour of marine soil when exposed to a “constant” temperature for a prolonged period of time. Accordingly, the constant desiccation test replicated field conditions where marine soil was exposed to the sun’s heat continuously without experiencing any form of moisture gain, which is commonly the situation during periods of minimal rainfall or drought where very little to no moisture reaches the soil.

2.6.1 Compacted specimens

Several past researchers have shown that shrinkage of compacted soils increase with increasing compaction water content [13, 41, 42, 54]. Hence in order to allow for a high shrinkage (as a conservative approach) while still remaining within the “acceptable compaction zone”, specimens were compacted to moisture contents of OMC + 4%. The compacted specimens were inserted into 50-mm diameter oedometer rings and placed in an oven to continuously dry at 60 °C (replicating temperature most likely experienced by soil upon exposure to solar radiation on the field) for several days. At the end of desiccation period, the specimens were removed from the oven and images of the top and bottom of the specimens were captured by a camera to analyse specimen deformation later using ImageJ software.

2.6.2 Slurry specimens

In addition to examining the desiccation behaviour of marine soil in its compacted state, it was necessary that its desiccation behaviour be analysed in slurry state as well, since the natural moisture content of marine clay when it was obtained was found to be quite high at an approximate 143%. Slurry specimens were thus prepared to a moisture content of 100% to investigate the desiccation cracking extent of marine soil when exposed to solar radiation at very high moisture content. Three specific batches of slurry mixtures were prepared in petri dishes. Each batch comprised NS, 1%, 2% and 4% BAS specimens. However, each batch was assigned a different biochar particle size range (i.e. PS-1, PS-2 and PS-3). The petri dishes were then placed in the oven at 60 °C for five days to simulate continuous exposure to solar radiation. The weights of the specimens were measured during the desiccation period. On the fifth day the specimens were removed from the oven and images of the slurry specimens’ top surfaces were captured by a camera to analyse the extent of desiccation cracking suffered by the specimens using ImageJ software.

2.7 ImageJ

ImageJ, a Java-based image processing program, was used to determine shrinkage in compacted soil specimens and the crack magnitude in slurry specimens, following subjection to thermal cycle and constant desiccation tests. For the area measurement, top and bottom images of the compacted specimens were captured using a camera. For each specimen, the average of the top and bottom surface areas was computed. Meanwhile, for the crack measurement in slurry specimens, only the top surfaces were captured since the specimens were unremovable from the petri dish without causing permanent damage to the specimen.

For each specimen, the “oval” tool was used to cover the circumference of the surface and measure the surface area of the specimen. The “create selection” option was used to select the cracked regions, and the “measure” option was employed to measure the areas of the selected cracked regions. The cracked area determined was subsequently divided by the total surface area of the specimen to obtain the Crack Intensity Factor (CIF) [34].

2.8 Determination of thermal properties

The KD2 Pro Thermal Properties Analyser was used to measure the thermal properties of unamended and amended soil specimens. The KD2 Pro device comprised a handheld controller and multiple sensors that were capable of being inserted into almost any material. For the present study, the SH-1 sensor was used to measure the thermal properties of the soil specimens. A total of six specimens were prepared for the test, viz. NS (PS-3), 1% BAS (PS-3), 2% BAS (PS-3), 4% BAS (PS-3), 2% BAS (PS-1), 2% BAS (PS-2). It was anticipated that the subjection of all four PS-3 specimens to the thermal property test would help gain an understanding on the variation of thermal properties with biochar amendment content. Alternatively, it was also expected that the subjection of PS-1, PS-2 and PS-3 specimens to the thermal property test would provide an insight into the variation of thermal properties with biochar particle size. The reasons for specifically choosing “2%” as the fixed biochar content to prepare BAS specimens with different particle sizes is because PS-3 2% BAS was considered to be the most economical amendment content for both areal and volumetric shrinkage reductions in compacted soils when exposed to the constant desiccation test. Furthermore, marine soil specimens amended with 2% content of PS-1 and PS-3 biochar particles respectively, were able to achieve minimum crack reduction in slurry form when subjected to the constant desiccation test. All soil specimens were compacted to their OMC values determined in the miniature compaction test series. Then the testing of each specimen was conducted using the KD2 Pro device.

2.9 Fourier Transform Infrared Spectroscopy (FTIR) analysis

A Fourier transform infrared spectroscopy (FTIR) analysis was carried out to examine the hydrophilic functional groups present in palm biochar particles. A specimen of powdered palm biochar particles passing 75 µm sieve was utilized for the test. Accordingly, a Nicolet iS10 (Thermo Scientific) spectrometer was used to obtain the spectra of using an average of 64 scans in the wavenumber range of

4000–400 cm^{-1} with spectral resolution of 4 cm^{-1} . Spectral outputs were recorded in the transmittance mode.

3 Results and discussion

3.1 Fourier transform infrared (FTIR) spectroscopy analysis

A FTIR analysis was run on a specimen of pure palm biochar to identify hydrophilic functional groups present within biochar so as to understand the affinity of palm biochar towards water. Accordingly, Fig. 2a shows the full FTIR result, while Fig. 2b and c portrays the two main transmittance peak regions of the FTIR graph as “section-A (S-A)” and “section-B (S-B)”, respectively. As depicted in Fig. 2b, the presence of a carbonyl group (C=O) was detected in the S-A region of the FTIR graph, which indicates the probable presence of specific organic compounds in biochar, viz., Carboxylic acids, Ketones, Aldehydes, Esters and/or Amides. Also, the detection of an amine group (N–H) in the S-A region of the FTIR result denotes the probable existence of a primary amine in biochar. Meanwhile, the recognition of a hydroxyl group (O–H) in the S-B region of FTIR graph signifies the plausible presence of a primary alcohol in biochar as well.

All three functional groups (i.e. C=O, O–H and N–H) detected in the FTIR graph have been reported as hydrophilic by past works [27, 40]. Accordingly, during experiments, the presence of hydrophilic functional groups in biochar would have enabled the biochar to absorb and retain a great quantity of water. Hussain et al. [20] stated that biochar intra-pores (micropores located within biochar particles) merely served as “storage regions” for the water molecules while the hydrophilic functional groups absorbed and retained the water molecules inside the pores. Kumar et al. [25] attributed the interaction between water molecules and hydrophilic functional groups to the well-known “hydrogen bonding” mechanism. Accordingly, Fig. 3 was developed to illustrate the potential ways that hydrogen bonds could form between the identified hydrophilic functional groups in biochar and its surrounding water molecules which would lead to the water retention within biochar [25, 43]. In Fig. 3, the black lines denote covalent bonds while the red dotted lines denote hydrogen bonds, where the letters, H, C, N, O and R refer to Hydrogen, Carbon, Nitrogen, Oxygen and rest of the molecule (group of carbon and hydrogen atoms), respectively. For ease of reference, the interaction between hydrophilic functional groups in biochar and its surrounding water molecules via hydrogen bonding mechanism would simply be referred to as the “functional group effect” in the subsequent sections.

3.2 Effect of biochar content on maximum dry density (MDD) and optimum moisture content (OMC)

Following the conduction of a series of mini-compaction tests, Fig. 4 highlights the variation of Maximum Dry Density (MDD) and Optimum Moisture Content (OMC) of the soil specimens with increasing biochar content. It is clearly seen that with increasing biochar content, the MDD and OMC of the specimens decreased and increased, respectively. This is a common phenomenon that has been observed by several researchers in the past. The MDD reduction observed in the BAS specimens could have been caused due to the replacement of natural soil particles by biochar particles that had a lower specific gravity (1.42) compared to that of natural soil (2.44). Alternatively, the MDD reduction may also have been caused by the increased porosity of BAS (compared to that of natural soil) due to the incorporation of highly porous biochar particles within the soil matrix. Consequently, at a given compaction energy, the entrapment of a higher volume of air in BAS pores most likely led to a reduced compressibility of the BAS specimens, which in turn, resulted in the BAS specimens being compacted at lower MDDs compared to that of natural soil [21].

Meanwhile, the increased OMC of the BAS specimens can be attributed to the higher water absorption and storage capacity of biochar particles (compared to that of natural soil particles) due to their highly porous structure, large specific surface area, substantial void ratio and functional group effect [20, 38]. The new inter-pores (micropores located between biochar–biochar and biochar–soil particles) and intra-pores introduced into the BAS matrix by fine biochar particles would have served as water storage regions, while water would have also adsorbed to the surface of the biochar particles in the form of films [9, 57]. Biochar has been known to function as a sponge that absorbs large volumes of water (more than ten times its own weight) as a combined result of its porosity and the functional group effect [20, 33, 66].

3.3 Effect of biochar content on thermal properties of compacted specimens

Figure 5a–c portray the thermal conductivity (TC), volumetric heat capacity (VHC) and thermal diffusivity (TD) trends of specimens amended with various PS-3 biochar contents. As depicted in Fig. 5a, the TC of BAS specimens reduced sequentially at low biochar contents (1–2%) but increased at a higher content of 4%. Nevertheless, the TC of all BAS specimens were lower than that of natural soil. Figure 4 clearly shows that the 1% and 2% BAS specimens

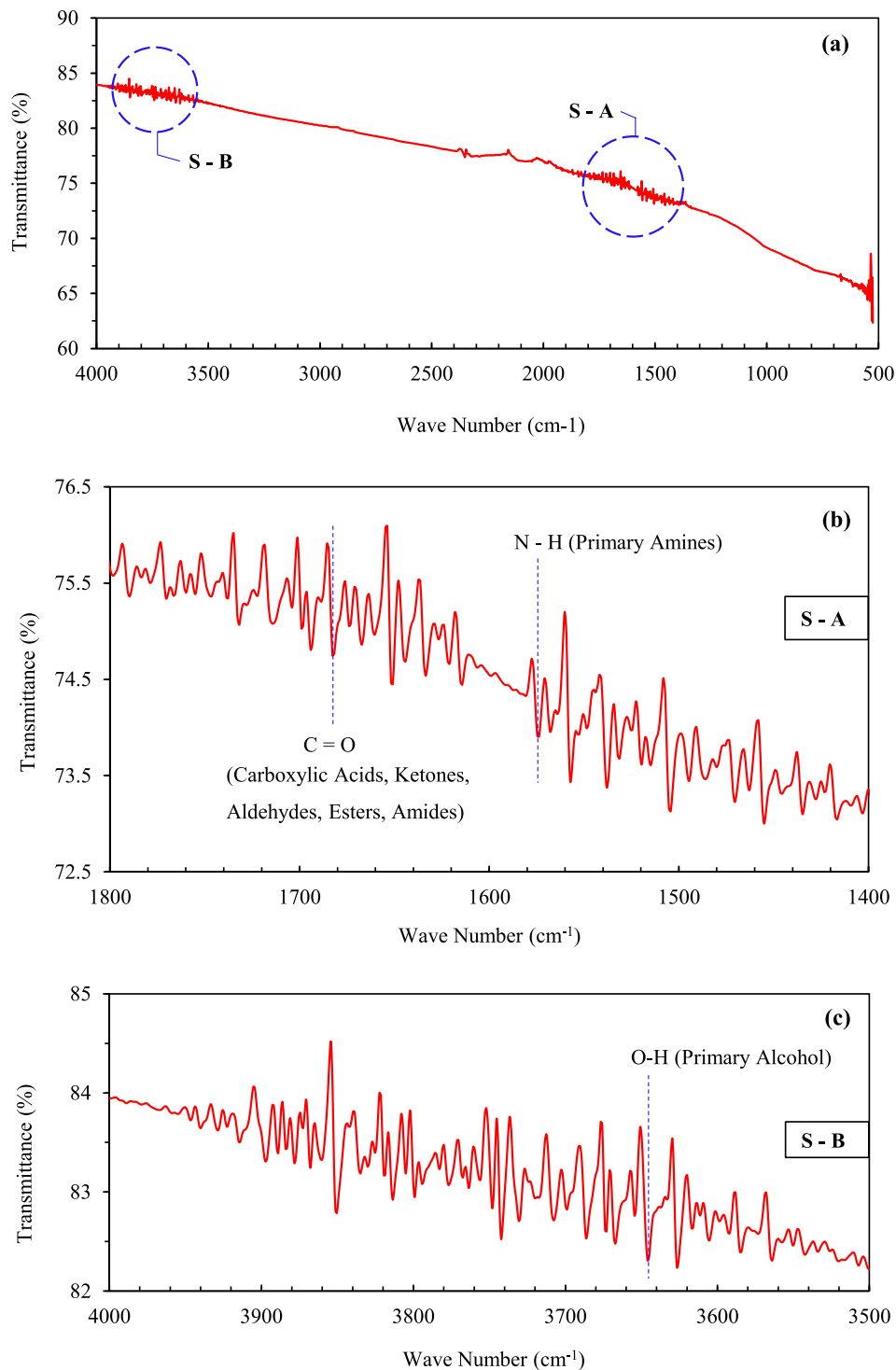


Fig. 2 Functional group detection in palm biochar using FTIR spectroscopy: **a** full FTIR result; **b** Section A (S-A); **c** Section B (S-B)

were compacted at lower MDDs compared to that of natural soil, due to the high porosity that existed in the BAS specimens. The increased porosity of the 1% and 2% BAS specimens (compared to that of natural soil) would have hindered the heat transfer across the BAS medium due to two reasons. Firstly, the presence of many voids/pores

would have led to a decreased connectivity between solid particles and reduced heat transfer via direct conduction. Secondly, the increased porosity would have resulted in a greater volume of air-filled pores within the BAS medium. Since the TC of air is one hundredth that of soil solids and water, heat transfer that occurred via

conduction/convection across the air that filled the pores would have been reduced [9, 31]. Alternatively, the inherently low TC of biochar itself may have also contributed to the reduced TC of the 1% and 2% BAS specimens [31].

Nevertheless, one may wonder why TC did not continue to decrease for the 4% BAS specimen as well, since its MDD was lower than those of 0–2% BAS specimens and

◀**Fig. 5** **a** Thermal conductivity variation with biochar content (PS-3); **b** volumetric heat capacity variation with biochar content (PS-3); **c** thermal diffusivity variation with biochar content (PS-3); **d** thermal conductivity variation with biochar particle size (2% BAS); **e** volumetric heat capacity variation with biochar particle size (2% BAS); **f** thermal diffusivity variation with biochar particle size (2% BAS)

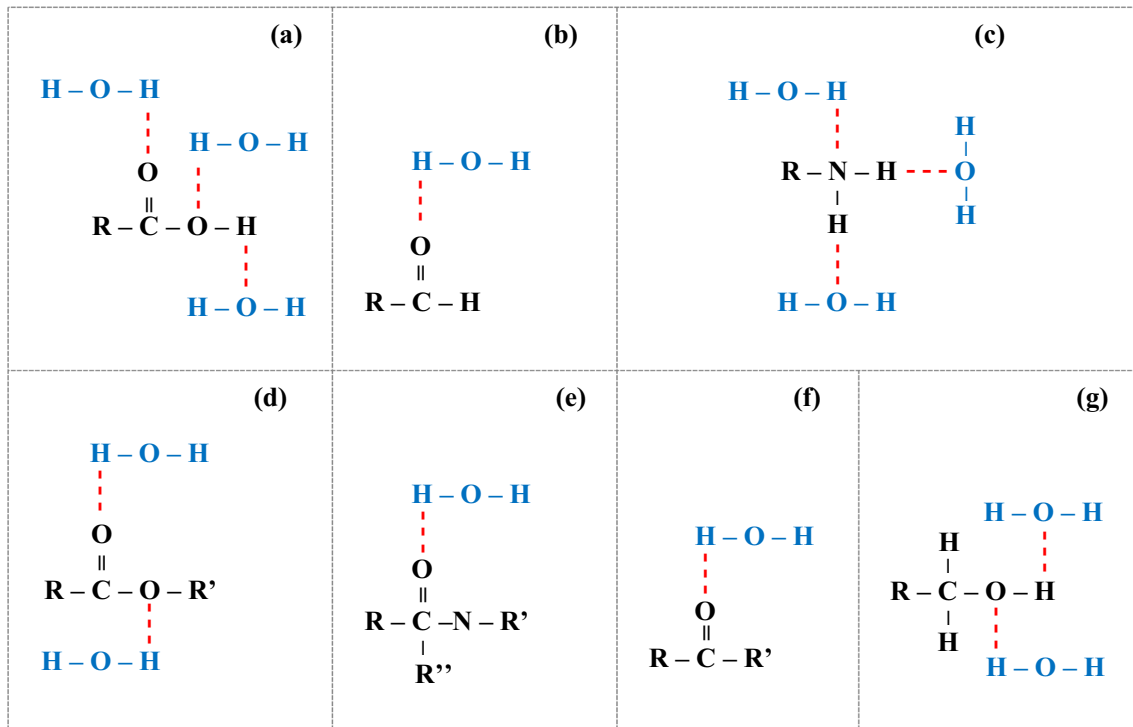


Fig. 3 Illustration of plausible hydrogen bonding mechanisms between water molecules and different classes of organic compounds in palm biochar: **a** carboxylic acid; **b** aldehyde; **c** primary amine; **d** ester; **e** amide; **f** ketone; **g** primary alcohol

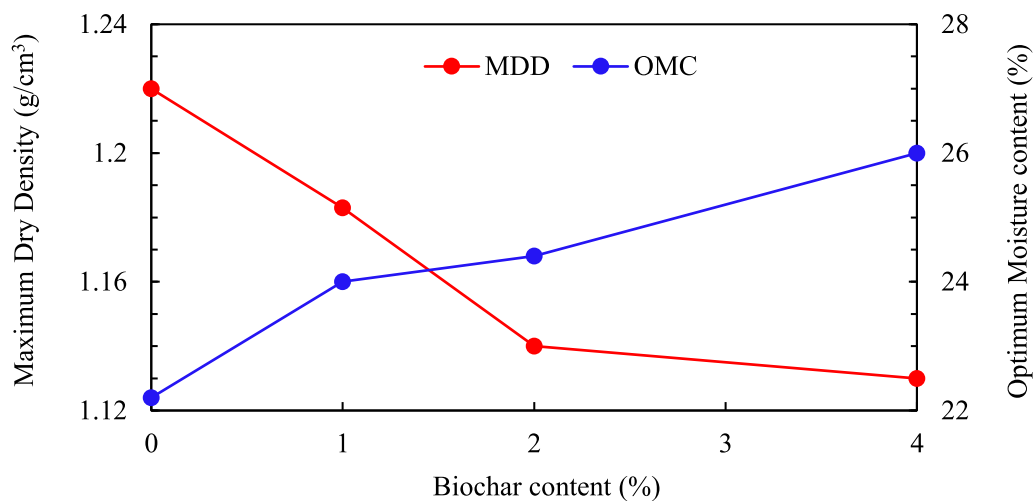
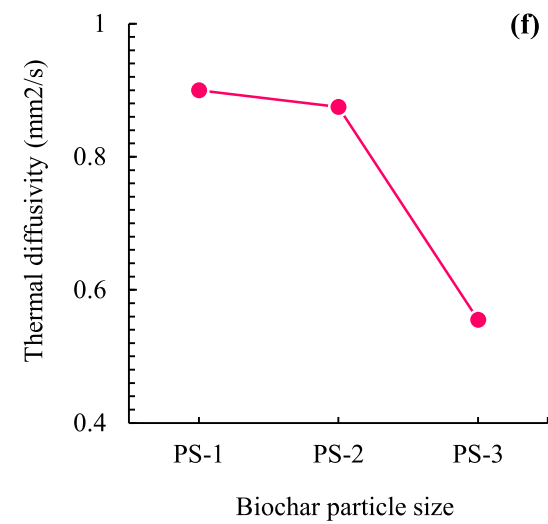
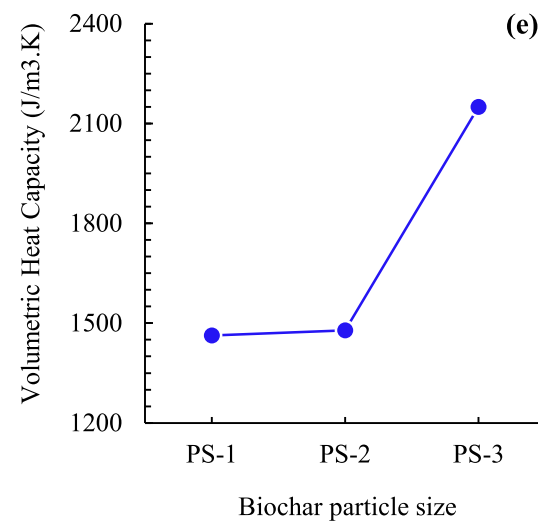
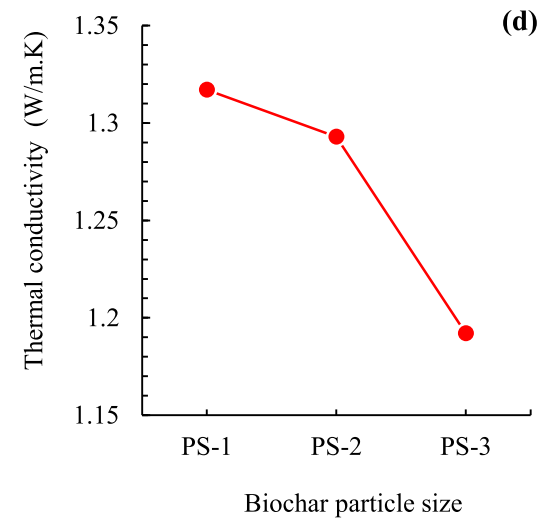
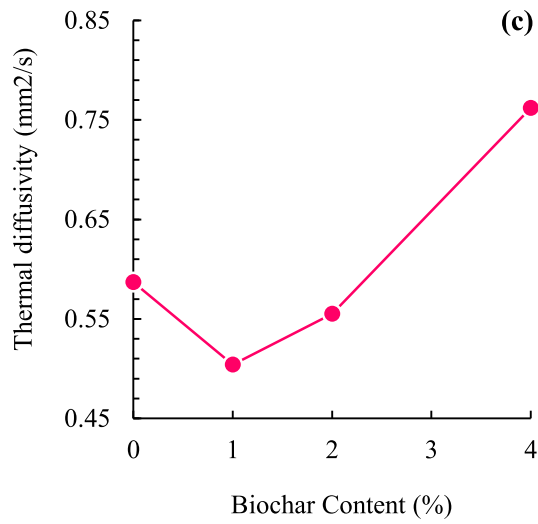
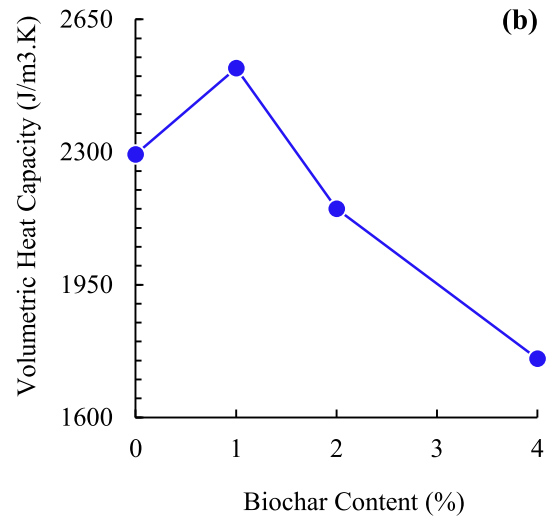
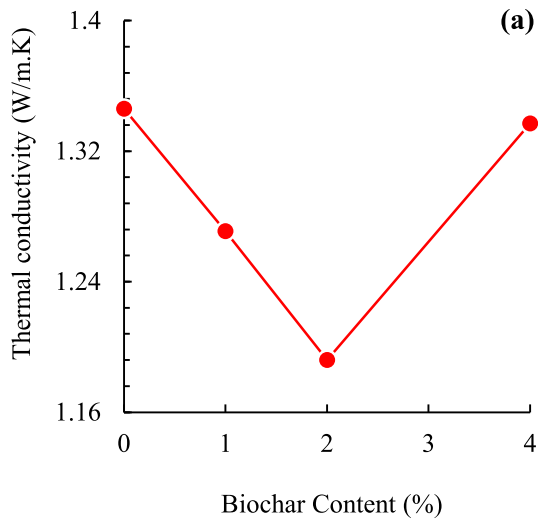


Fig. 4 Maximum dry density (MDD) and optimum moisture content (OMC) of all specimens



since it also contained the greatest quantity of (low thermal conductive) biochar among the BAS specimens. This is because, in addition to MDD and porosity, water content also played a major role in altering the thermal properties of the BAS. As per Fig. 4, the water content of BAS rose with increasing biochar content. It is a well-known fact that as the quantity of water within a soil medium increases, its TC also rises dramatically. This is because the water particles form films around the solid (biochar and soil) particles increasing the contact area between the solid particles [1]. Therefore, the high TC of 4% BAS can be attributed to its higher volume of water content, which presumably increased the connectivity between solid particles [9]. If carefully analysed, Fig. 5a shows that a close battle existed between the individual contributions of MDD, porosity and water content towards the alteration of BAS TC. It is apparent that the effects of low MDD and high porosity dominated over the high water content effect in the lower biochar content range. However, at a higher biochar content, the effect of increasing water content evidently governed the TC variation in BAS. This could mean that although at 4% biochar content, there was high porosity and low MDD in the BAS, the high volume of water present formed films around the soil and biochar particles which in turn led to an improved connectivity between them. The increase in heat transfer caused by this enhanced connectivity between solid particles by water was evidently sufficient to outweigh the reduction of heat transfer caused by high porosity, low MDD and the inherent low TC of biochar.

Figure 5b exhibits the VHC trend which rises for the 1% BAS specimen and then drops for the 2% and 4% contents. Fröb [16] defined the VHC of a soil system as the sum of the VHCs of the individual soil constituents weighted by their respective volumetric contents. The soil/BAS constituents in this case include air, water, soil and biochar. According to Liu et al. [31], the volumetric heat capacity of water is far higher than the average volumetric heat capacities of soil mineral and organic particles. Therefore, the sudden rise in VHC observed for the 1% BAS can partly be ascribed to its high water content compared to that of natural soil. Alternatively, Liu et al. [31] revealed that the volumetric heat capacity of pure biochar was higher than the average volumetric heat capacities of soil mineral and organic particles as well. Hence, the introduction of biochar into the soil matrix may also have contributed towards an increase in VHC of 1% BAS. However, it seems that for the 2% and 4% BAS, the increased porosity and low MDD would have led to a decrease in the BAS VHC due to the presence of more air-filled pores. According to Liu et al. [31], VHC of the air that fills the pores of the BAS is significantly lower than

those of water, pure biochar, soil mineral and organic particles.

However, the question then arises as to why the water content that 4% BAS possessed was high enough to increase its TC, but not its VHC. The authors believe that this phenomenon could be explained using Fig. 6a and b, which depict the hypothesized particle arrangements for 1% and 4% BAS specimens, respectively. The water films around the biochar and soil particles would have been thinner in 1% BAS compared to 4% BAS, since 4% BAS possessed a relatively higher water content. Furthermore, the porosity of the 1% BAS matrix would have been lower compared to 4% BAS, since at such a low content, the fine biochar would have filled the inter-pore spaces between soil particles and reduced porosity. Contrastingly, the

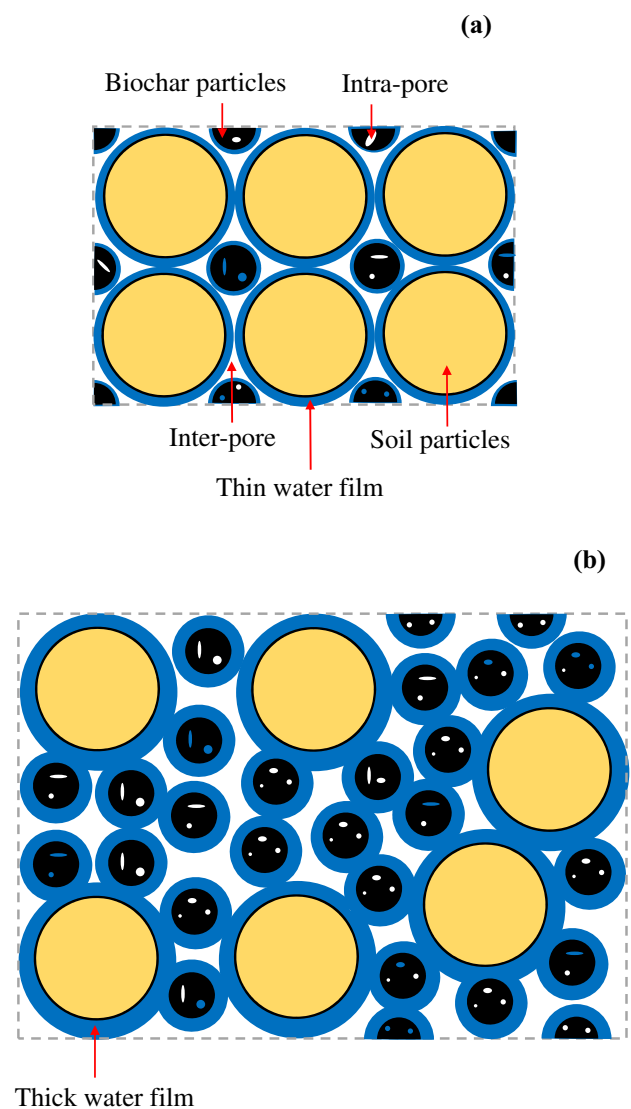


Fig. 6 Hypothesized representation of BAS particle arrangement: **a** inter-pore filling by few PS-3 biochar particles (1% BAS); **b** increased porosity by excess PS-3 biochar particles (4% BAS)

excessive number of intra-pores and inter-pores introduced into the soil matrix owing to the incorporation of a *large* content of fine biochar particles would have altered the pore structure and led to 4% BAS having a higher porosity than that of 1% BAS [60]. Meanwhile, the additional volume of water that 4% BAS possessed compared to 1% BAS, would not have been sufficient to fully intrude the air-filled pores and replace all of the air within the pores. Instead, the additional water quantity in 4% BAS would most likely have replaced the air around the surfaces of the solid particles by increasing the water film/hull thickness, which in turn would have increased the connectivity between the solid particles. Therefore, while the increased connectivity would have resulted in 4% BAS having a higher TC than 1% BAS, its higher porosity would have still led to a lower VHC due to the air (present within the pores) possessing a low VHC [9, 31].

Figure 5c shows that TD decreased for 1% BAS and then increased for the rest of the biochar contents. TD is generally considered as the ratio of the TC and VHC [1]. Hence, it is safe to assume that the factors responsible for causing the variations in TD of a specimen are entirely included within the factors that caused variations in the TC and VHC of the specimen. Based on the trend depicted in Fig. 5c, at 1% biochar content, the decrease in TC and increase in VHC would have caused an immediate decrease in TD. At 2% content, even though TC continued to decrease, the sudden drop in VHC would have been significant enough to reverse the direction of the TD trend and cause it to rise. Finally, at 4% BAS, the decrease in VHC and rise in TC would have led to an increase in TD as per the nature of the relationship between the three properties.

3.4 Effect of biochar particle size on thermal properties of compacted specimens

Figure 5d–f illustrate the effect of biochar particle size on the thermal conductivity (TC), volumetric heat capacity (VHC) and thermal diffusivity (TD) of the 2% BAS specimens. The declining TC trend depicted in Fig. 5f can be attributed to the relationship that exists between thermal resistivity of the BAS medium and the size of solid particles that constitute the medium. For the sake of comparison among the PS-1, PS-2 and PS-3 BAS specimens, it is assumed that the soil particle size was nearly the same for all three specimens and that the main disparity between them was caused by the difference in biochar particle size incorporated. For maximum comparison effect, Fig. 7a–c shows the hypothesized heat flow paths for only the specimens incorporated with the largest (PS-1) and smallest biochar particle ranges (PS-3). Nevertheless, the mechanism discussed would still be applicable to the PS-2 specimen as well.

The number of physical contact points between the biochar–biochar and biochar–soil particles would have increased rapidly when the biochar particle size decreased. This effect has been shown in an exaggerated manner via Fig. 7a and b for ease of understanding. The biochar particles in Fig. 7b are merely illustrated in an orderly arrangement to highlight the increase in contact points between the PS-3 biochar–biochar particles compared to a single biochar particle in PS-1. The increased number of contact points would have narrowed the heat flow path and reduce heat flow (denoted by red arrows) between particles as a result of increased thermal resistivity due to limited contact area for heat transfer at the physical contact points [64]. Moreover, as depicted in Fig. 7c, fine biochar particles in PS-3 would create a more tortuous voids structure compared to PS-1, which would once again hinder the heat flow and increase thermal resistivity within the PS-3 BAS system [22]. Red arrow thickness represents the heat flow magnitude, where the thin red arrows indicate reduced heat flow at limited particle contact points. Hence, due to increased thermal resistivity by presence of fine particles, the thermal conductivity was observed to decrease with decreasing biochar particle size.

Figure 5e shows that the VHC increased with the reduction of biochar particle size. With decreasing particle size, the external specific surface area (SSA) of biochar particles would have increased [9, 28]. The increased external SSA would have led to finer biochar particles being able to adsorb a greater quantity of water molecules that possess a high VHC (due to the functional group effect) along its surface, forming thick water hulls/films compared to large biochar particles, which may have led to the BAS system with finer biochar particles having a higher VHC compared to a BAS system with coarse biochar grains [1, 9]. Moreover, coarse biochar particles would have had more intra-pores compared to the fine particles since grinding of biochar into fine particles would have led to the destruction of a significant quantity of its intra-pores [20]. Consequently, the presence of a higher number of intra-pores would have increased the probability of air being trapped within the pores and led large biochar particles to have more air-filled intra-pores compared to the finer particles. The presence of a higher quantity of air-filled pores may have therefore led to a lower VHC in BAS systems with large biochar particles since the VHC of air is lower than that of water, pure biochar, soil mineral and organic particles [31]. Figure 5f shows that the thermal diffusivity (TD) of BAS specimens decline with a reduction of biochar particle size at a constant content of 2% biochar. Since the TD is considered as the ratio of TC and VHC [1], it can be inferred that the factors that caused variations in TC and VHC of the BAS specimens were responsible for causing the observed change in TD as well.

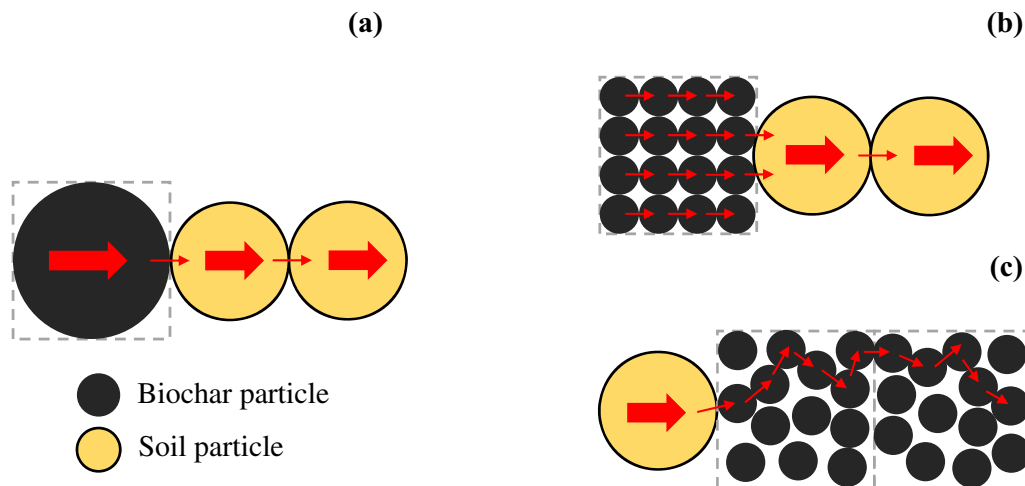


Fig. 7 Hypothesized heat flow representation across BAS particle arrangement: **a** few particle contact points and a relatively direct heat transfer (PS-1); **b** many particle contact points (PS-3); **c** tortuous heat transfer path (PS-3). Note: Red arrows denote heat flow based on the thermal resistivity faced in its pathway

Given the relationship between TC, VHC and TD, the trend of TD portrayed in Fig. 5f is predictable and agrees well with the trends of both TC and VHC.

3.5 Effect of thermal cycles on deformation of compacted specimens

Figure 8 demonstrates the volumetric deformation of compacted natural soil (NS) and PS-3 BAS specimens with increasing thermal cycles. The change in volume of all

specimens have been plotted with respect to their “initial compacted volumes” (volume of specimens before the first wetting phase), while W_n and D_n denote “n” number of “wetting” and “drying” phases, respectively. The equation used for calculating Absolute Volumetric Deformation for a specimen is provided below as Eq. (1), where V_n and V_i refer to the “volume of specimen after a wet or dry phase” and “initial compacted volume of specimen”, respectively.

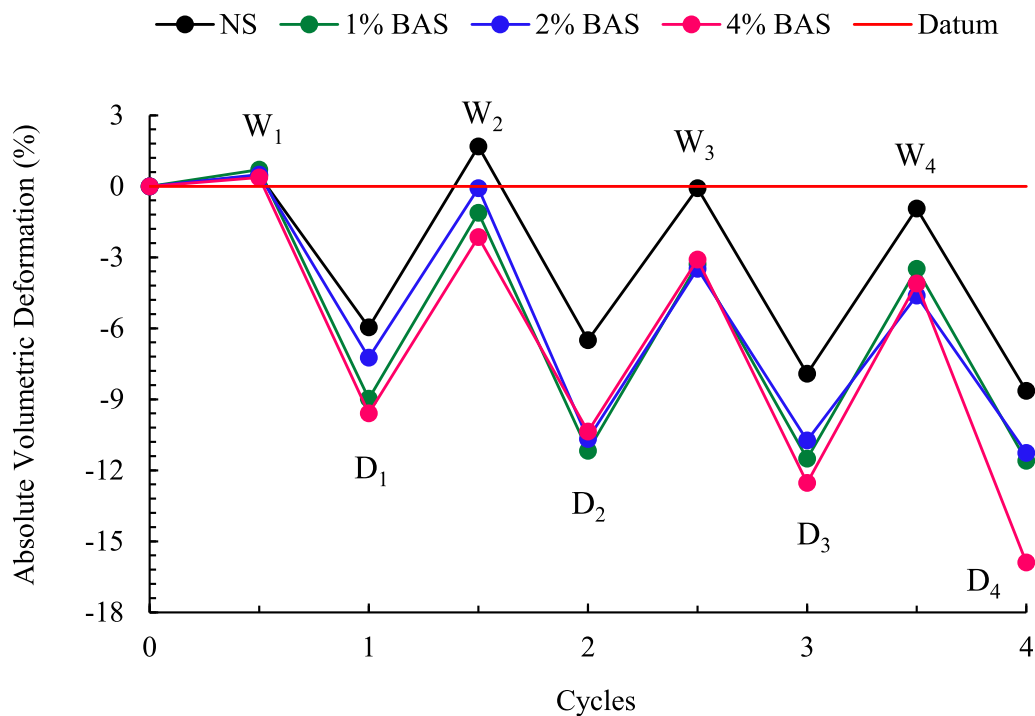


Fig. 8 Absolute volumetric deformation of all specimens subjected to thermal cycles

$$\text{Absolute Volumetric Deformation}(\%) = \frac{V_p - V_i}{V_i} \times 100 \quad (1)$$

Figure 8 shows that the volume deformation calculated for the first wetting phase was smaller for all specimens compared to the rest of the wetting phases. This is predictable since prior to the first wetting phase, each specimen's diameter was equivalent to that of its respective oedometer ring. Hence, the lateral expansion of all specimens was very much restricted during the first wetting phase and the volumetric deformation was mainly caused by the axial swell. However, the rest of the wetting phases were always preceded by a drying phase and as a result, the specimens' diameters (prior to wetting) were smaller than the oedometer ring's diameter due to their shrunk areas. This allowed specimens to swell both axially and laterally until their boundaries came into contact with the oedometer rings' walls, which consequently led them to experience higher volumetric deformations.

Alternatively, Fig. 9a–d denote the initial wetting moisture contents that NS, 1% BAS, 2% BAS and 4% BAS possessed prior to being subjected to each wetting phase. It

is evident that while the specimens' initial wetting moisture contents of the 2nd, 3rd and 4th wetting phases did not vary significantly among themselves, they were substantially lower than the initial wetting moisture content of the first wetting phase. It is a well-known fact that a *drier* soil swells more than a *wet* soil. This is mainly due to the presence of a high matric suction in the soil/BAS matrix at low water contents, which increases the affinity of the soil/BAS matrix towards water that in turn leads to high swelling [35]. Hence, there is a possibility that the significant difference in initial wetting moisture contents led specimens to expand/swell more in the 2nd, 3rd and 4th wetting phases compared to the 1st wetting phase.

While all specimens underwent volume deformation, no visual cracks were observed on any specimen even after consecutive subjection to 4 thermal phases. This maybe caused due to several factors. Fundamental crack mechanics dictate that for cracks to be developed, the shrinkage strain of the soil matrix (that results from high matric suction developed in its pore structure during drying) needs to be “restrained”. When the shrinkage is restrained, high tensile stresses would develop within the soil matrix which would ultimately lead to “desiccation

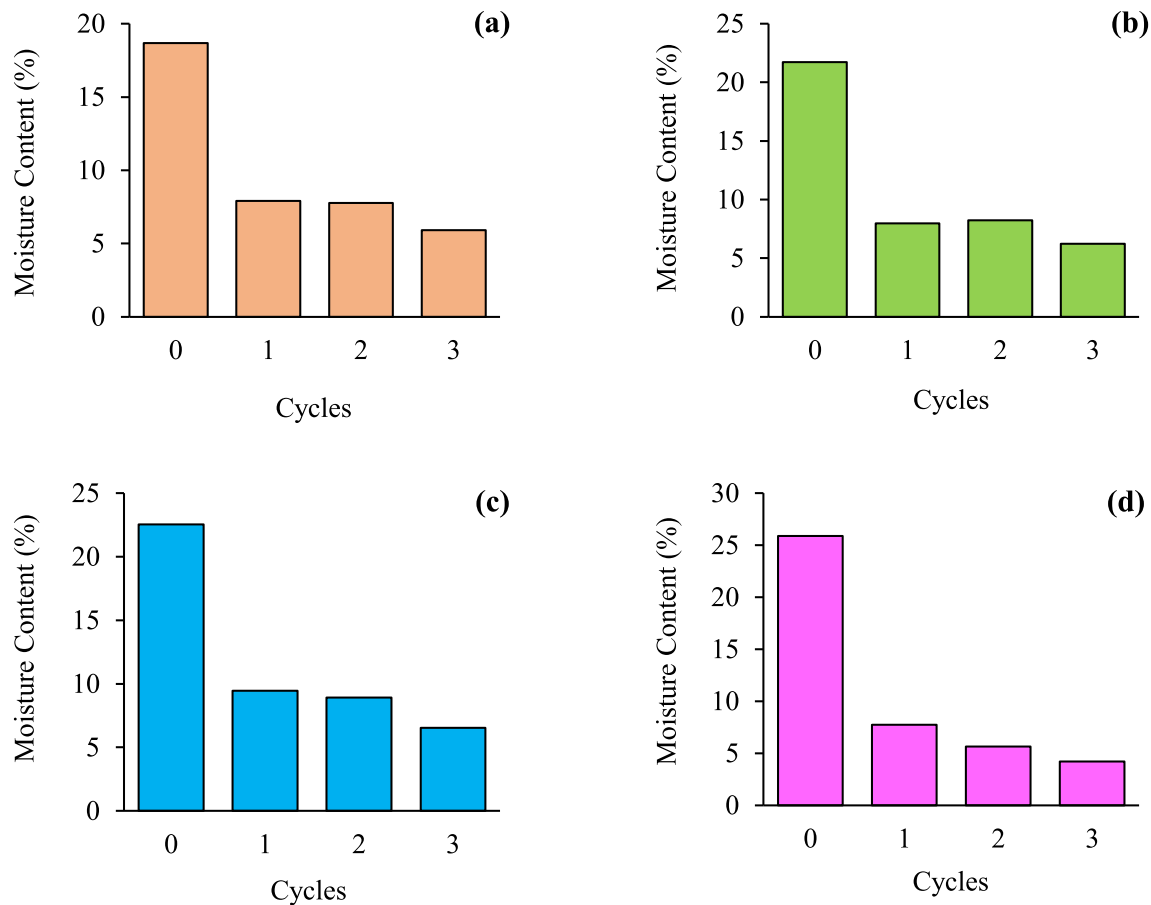


Fig. 9 Moisture content prior to commencement of each wetting cycle a NS, b 1% BAS, c 2% BAS, d 4% BAS

cracking” of the soil once its tensile strength is exceeded at some point [37]. In the thermal cycle series, the fact that all specimens experienced high volume deformations (both axially and laterally) during drying, while not cracking in the process, could be attributed to the unrestrained, free shrinkage allowed by the smooth ring walls to the specimens [4]. Moreover, since the drying period was limited to approximately 7 h for each drying phase, the moisture loss may not have been sufficient to create high matric suction values within the soil matrix and lead to desiccation cracking [11].

Figure 8 also shows that, from the 3rd wetting phase onwards, all specimens were unable to reach their initial compacted volumes following wetting. This observation is further highlighted in Fig. 10, which displays the trends for only the volumetric swell deformations of all specimens after each wetting phase. The absolute volumetric swell was calculated using Eq. (2), where V_{sp} and V_i refer to the “volume of a specimen after a specific swelling phase” and “initial compacted volume of a specimen”, respectively.

$$\text{Absolute Volumetric Swell (\%)} = \frac{V_{sp} - V_i}{V_i} \times 100 \quad (2)$$

For BAS specimens in particular, Fig. 10 shows that after the very first thermal cycle itself, their volumes after each swelling phase became lower as the number of cycles increased. For natural soil, the same phenomenon was observed after the second thermal cycle. This may have been caused by an irreversible deformation in the soil or soil–biochar fabric due to rearrangement of soil/biochar particles and destruction of pore microstructure, following

subjection to continuous wetting and drying phases [61]. Basma et al. [7] stated that during wetting and drying cycles, the quantity of voids within the soil system reduces which mitigates the ability of the soil to gain more water upon further wetting, which in turn reduces its ability to increase its volume. According to [49], in the initial state, the clay content of a soil specimen is present within the soil matrix in the form of weak thin sheets/layers which has the ability to absorb a significant quantity of water. However, upon subjection to continuous wetting and drying phases, the layers lose their initial structure and become connected to one another which reduces their water absorption capacity and in turn, reduces the ability to expand.

Figure 13 shows the absolute axial deformations of the specimens with increasing thermal cycles. The absolute axial deformations are calculated the same way as the Absolute Volumetric Deformation (%) using Eq. (1), except that the volume dimensions are replaced by the height dimensions. Similar to Figs. 8 and 10, Fig. 11 also confirms the irreversible deformation behaviour of all specimens after the first two cycles. Consequently, this insinuates that both natural soil and BAS when compacted on the field, would ultimately settle to a height lower than its initial compacted height if exposed to continuous thermal cycles, which would evidently serve as a threat to the overlying structures. Figure 12 highlights the Absolute Volumetric Shrinkage of the specimens calculated with respect to their initial compacted volumes (measured prior to being subjected to any thermal cycle), using Eq. (3), where V_{dp} and V_i refer to the “volume of a specimen after a

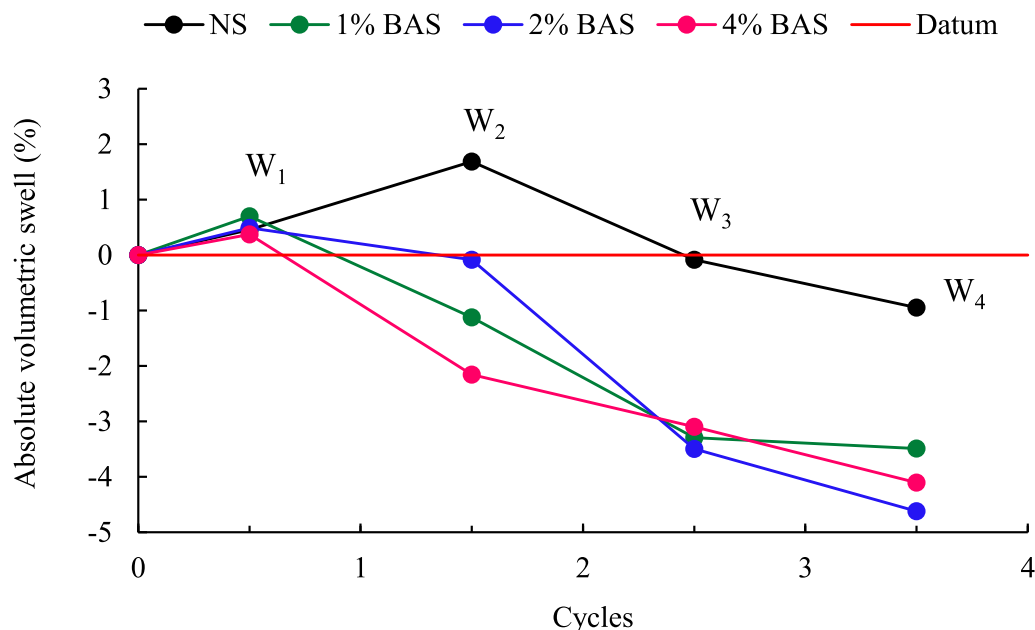


Fig. 10 Absolute volumetric swell deformation of all specimens with thermal cycles

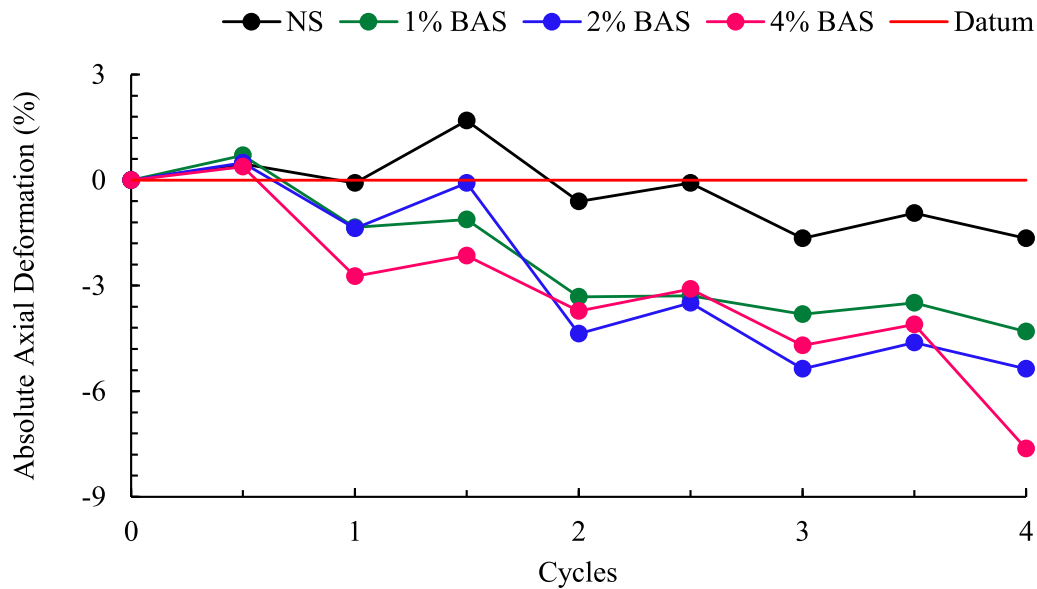


Fig. 11 Absolute axial deformation of all specimens with thermal cycles

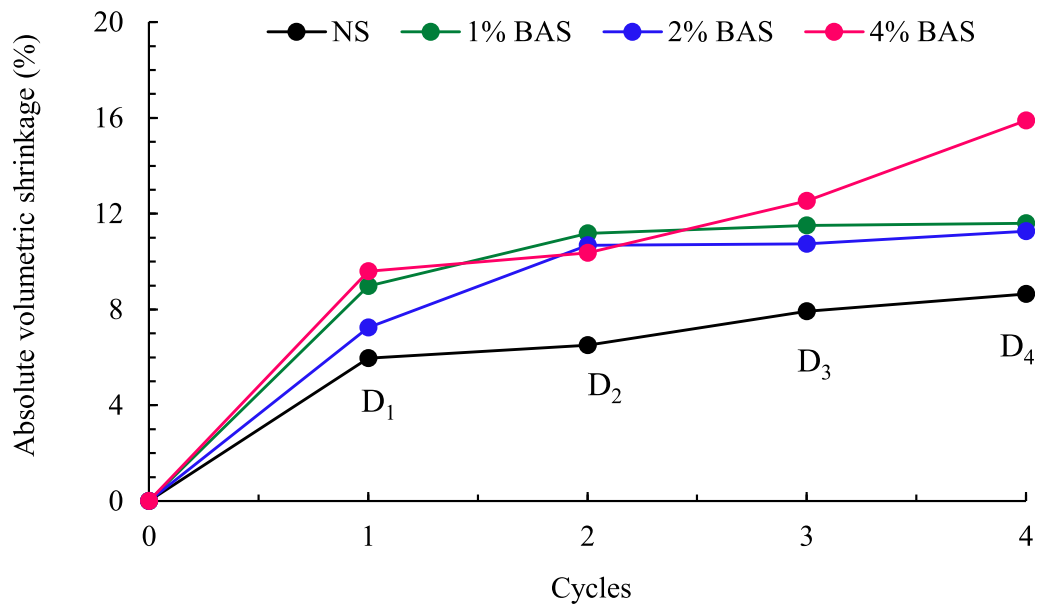


Fig. 12 Absolute volumetric shrinkage of all specimens with thermal cycles

specific drying phase” and “initial compacted volume of a specimen”, respectively.

$$\text{Absolute Volumetric Shrinkage (\%)} = \frac{V_{dp} - V_i}{V_i} \times 100 \quad (3)$$

Figure 12 shows that the absolute volumetric shrinkage increases with increasing number of thermal cycles irrespective of the biochar amendment levels. If analysed closely, it is perceived that for all specimens, the shrinkage effect on the BAS matrix was arguably the most significant during the first drying phase. Afterwards, even though

shrinkage deformations increased with the number of cycles, the additional shrinkage that the specimens experienced when exposed to new drying phases were not as significant compared to the shrinkage experienced during the first drying phase. For example, the absolute shrinkage deformation experienced by 1% BAS after the first drying phase was 8.9%, whereas after 4 times the number of drying phases, it still experienced only 11.5% shrinkage which was only 2.6% higher. This phenomenon is understandable, given the high moisture content the specimens possessed immediately after compaction. Loss of a high volume of water from voids during the first drying phase

would have definitely resulted in a significant decrease in voids content, irreversible particle rearrangements/fabric changes and breakage of particle bonds [36]. Upon rewetting, the rearranged soil/BAS matrix would have been further weakened by the addition of water due to the softening of particle rigidity [62]. Subsequently, subjecting the weakened specimen to drying once again would have then caused it to become weaker and shrink even further. This process would have repeated for the rest of the thermal cycles. According to Albrecht and Benson [3], high volumetric shrinkage strains during the first drying phase indicates that the inter-particle stress applied by suction to the specimens during drying was much higher than the stress applied to them during their compaction. Figure 12 shows that BAS specimens shrunk more compared to the natural soil. Once again, this is predictable given the high water retention capability of fine biochar particles. The high affinity of biochar for water was already reflected from the OMC trend portrayed in Fig. 4. Since fine biochar particles would have possessed a large specific surface area, hydrophilic functional groups and increased the number of micropores within the BAS matrix, a higher volume of water would have been stored within the BAS specimens during the wetting phases [9, 20]. Garg et al. [17] stated that clay particles could fill the available intrapores that exist within the biochar particles which would lead to the reduction of biochar's pore throat diameters and a 40% increase in the volume of water retained within the BAS specimen. No specific trends were recognized among the biochar contents with respect to shrinkage or swelling in the thermal cycle series. Even if such trends would have existed, they might have been concealed by the effects of repeated wetting and drying phases on the soil specimens. Nevertheless, it was revealed that the biochar amendment in particular, did not aid in improving the behaviour of marine soil in the face of repeated "thermal cycles".

3.6 Effect of biochar content on shrinkage of compacted specimens under constant desiccation

Figure 13 shows that under constant desiccation, both the volumetric and areal shrinkage of compacted specimens decreased with increasing PS-3 biochar percentage. The reduction was significant between 1 and 2% biochar contents. The volumetric shrinkage and areal shrinkage of each specimen was calculated using the below equations, where V_i , V_f , A_i , A_f refer to initial volume, final volume, initial area and final area of the specimen, respectively.

$$\text{Volumetric shrinkage (\%)} = \frac{V_f - V_i}{V_i} \times 100 \quad (4)$$

$$\text{Areal shrinkage (\%)} = \frac{A_f - A_i}{A_i} \times 100 \quad (5)$$

Overall, among the tested specimens, the maximum shrinkage reduction was achieved by 4% BAS. Accordingly, compared to natural marine soil, 4% biochar amendment attenuated the volumetric and areal shrinkages by 42% and 47%, respectively. However, 2% BAS was still able to achieve 34% and 44% reductions in volumetric and areal shrinkages despite employing half the content of biochar compared to 4% BAS. For the small-scale laboratory experiments, the mass difference between 2 and 4% biochar contents would seem insignificant. However, when used in the field for large-scale projects, the difference between the two biochar quantities would be substantial and using 4% biochar content may not be economical in terms of biochar material and transportation costs.

Several researchers in the past such as Cuilan et al. [12], Malongweni et al. [33], Villagra-Mendoza [57], Zong et al. [67] have also observed that inclusion of various contents of biochar in natural soil led to significant attenuations in its shrinkage behaviour. Cuilan et al. [12] reported that biochar amendment lessened the shrinkage by as much as half its original capacity. Villagra-Mendoza [57] observed that with increasing biochar amendment, less shrinkage occurred in both vertical and horizontal directions of the specimen. Villagra-Mendoza [57] attributed this behaviour to biochar acting as a binding agent which resulted in a more rigid soil structure. Hence, the more biochar employed, the more rigid the BAS matrix became and the more resilient the BAS system was against drying. Villagra-Mendoza [57] also stated that the high surface area of biochar particles enabled them to adsorb and retain a significant volume of water in the form of films around the particles even under high matric potentials, which led to reduction of both pore stress and volumetric deformation. Meanwhile, Zong et al. [67] ascribed the shrinkage reduction to a change in the shrinkage properties of clay minerals caused by the influence of carbon particles introduced into the soil matrix by biochar. The interaction between the carbon (C) particles of biochar and clay colloids of the soil would result in the formation of clay-C complexes which would influence the particle behaviour within the BAS system at a colloidal level. This would in turn cause substantial changes at the microstructural level and affect shrinkage properties of the BAS system.

The particle size of biochar employed for the desiccation test was below 75 μ m. Hence, when introduced into the natural soil, such fine biochar particles would have evidently filled and clogged the wide pores (macropores) present within the soil matrix. This would have led to a decrease in the number of coarse pores and a consequent increase in the number of mesopores within the BAS

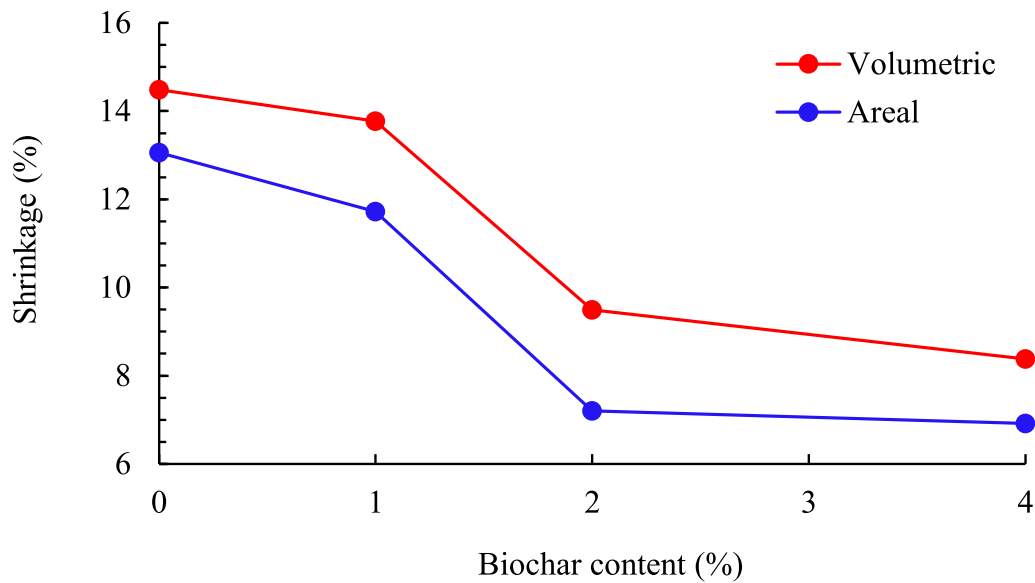


Fig. 13 Volumetric and areal shrinkage variation of specimens under constant desiccation

matrix. Additionally, the intra-pores present within the biochar particles would have contributed to the increased number of micropores within the BAS system as well [57]. Presence of a high quantity of narrow pores (mesopores and micropores) within the BAS matrix would have limited the volume contraction by limiting the escape/loss of water during drying. Strong forces that resulted from capillarity together with the functional group effect would have held water tightly within narrow pores and not allowed it to escape easily during desiccation [20, 25]. Moreover, the lower thermal conductivity of BAS compared to that of natural soil would have led to attenuated heat transfer across the BAS matrix, which in turn would have lowered water evaporation and resulted in reduced shrinkage.

3.7 Effect of biochar content on evaporation in compacted specimens under constant desiccation

The weights of the compacted specimens measured during drying were used to plot the cumulative moisture loss over time (Fig. 14a). Subsequently trendlines were included in the moisture loss plots and evaporation rates were also calculated for the specimens by taking the gradient of the moisture loss curves. It would be quite unfair to compare the total volume of moisture loss that occurred between specimens at the end of the drying period, since the initial compacted moisture contents were different for each specimen prior to drying. Instead, it was deemed fairer that the moisture variation between the specimens be discussed in terms of evaporation rates. Accordingly, Fig. 14b highlights the specimens' evaporation rates for the first 30 h since after approximately 30 h, the moisture variation was

minimal. Figure 14b clearly shows that the natural soil (NS) experienced the highest initial evaporation rate, while the PS-3 BAS specimens showed lower rates. The evaporation rates of both natural soil and 1% BAS dropped drastically (with steep slopes) within the first 10 h signifying that majority of the water loss occurred within the first 10 h of drying. Conversely, both 2% BAS and the 4% BAS specimens showed more controlled evaporation rates with mild slopes throughout the 30-h period. Upon heat application, the water located in the pores present within the soil specimen's top region evaporated and over time, the water available at the lower regions of the soil was carried to its surface via capillarity depending on the quantity of narrow pores present within the soil/BAS matrix. As the drying time progressed, the quantity of water available for evaporation diminished gradually which led to a reduction of pore water connectivity and capillary action, which in turn resulted in a decreased evaporation rate [60]. The fact that only a minor difference existed between the evaporation rates of NS and 1% BAS shows that the application of a biochar content as small as 1% was insufficient to control the moisture loss in soil during rapid drying at elevated temperatures compared to the contents of 2% and 4%.

The more controlled evaporation rates of BAS specimens compared to the natural soil could be attributed to a variety of factors. Firstly, as mentioned earlier in this paper, the addition of fine biochar would have clogged and reduced the size of coarse pores (macropores) present within the natural soil matrix which would have in turn increased the quantity of micropores present within the BAS matrix. Such narrow pores would have held the water molecules tightly and limited their escape owing to the

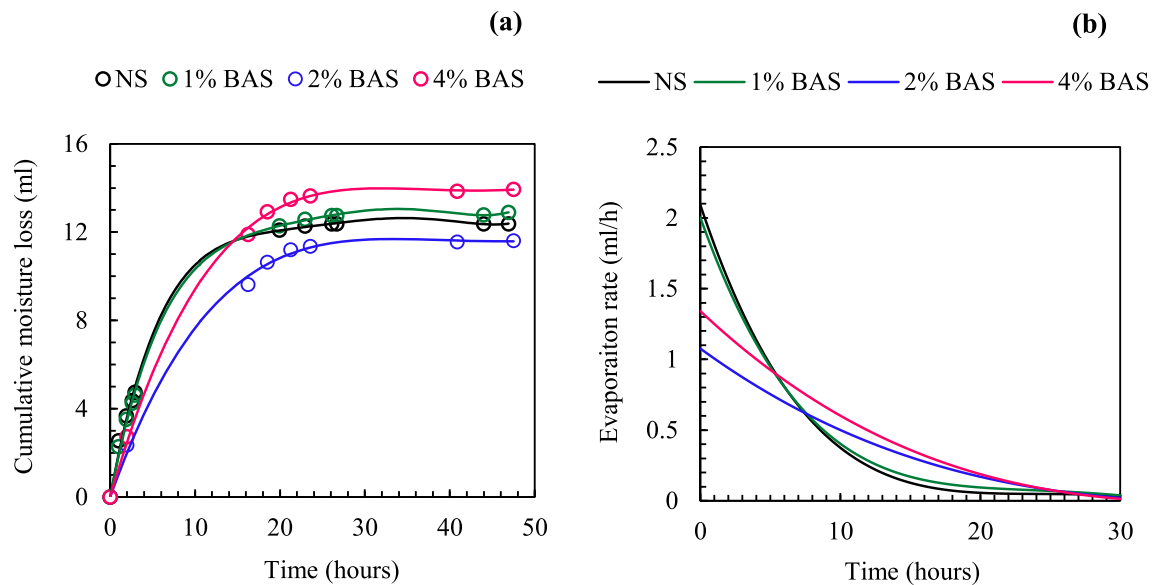


Fig. 14 Moisture variation in compacted specimens during drying: **a** cumulative moisture loss; **b** evaporation rate

functional group effect and forces resulting from capillarity [20, 25, 57]. Secondly, the clogging of wide pores by fine biochar would have evidently reduced the formation of effective water migration channels and hindered the water flow up to the surface for evaporation [9, 30, 65]. Thirdly, inclusion of biochar grains within the soil matrix would have created tortuous interstitial spacing between the soil and biochar particles which would have resulted in low hydraulic conductivity of the specimen. Presence of low hydraulic conductivity would have then aided to hamper the transport of water up to the surface for evaporation [6]. Finally, the low thermal conductivities of 2% and 4% BAS compared to natural soil would have led to attenuated heat flow across the BAS matrix and reduced water loss. The steep slope of natural soil's evaporation rate indicates that the water present within the soil matrix was easily available for evaporation and hence escaped in large quantities within the first few hours itself, whereas for BAS specimens with high biochar percentages, significant rates of evaporation lasted for a longer period of time compared to natural soil since the water available within the BAS matrix was not easily allowed to evaporate due to the intervention of the biochar particles.

Interestingly however, 4% BAS exhibited a higher evaporation rate than 2% BAS. This once again, could have been caused due to several reasons. Firstly, if the quantity of biochar is increased beyond a certain threshold, its inherent porosity would begin to negatively affect the characteristics of the amended soil. Since biochar is a porous substance, once it is included in "excessive" amounts within the soil matrix, even if the specimen is compacted, the BAS mixture is not easily compressed, and

the porosity of the BAS will consequently rise due to the increased number of micropores [60]. Secondly, addition of a higher quantity of biochar would have presumably led to an increase in the magnitude of functional groups in the BAS matrix as well. Accordingly, increased porosity and functional group effect in 4% BAS would have enabled it to hold a higher quantity of water than 2% BAS, so that more water would have been available for evaporation. Thirdly, the introduction of an "excessive" quantity of micropores would have led to the formation of well-connected narrow flow channels along the interstitial space of the soil matrix and within the biochar particles themselves. This would have consequently increased both the hydraulic conductivity and capillary effect in the flow pathways which would have enhanced the transport capacity of water to the surface and promoted evaporation [6, 20, 60, 65, 66]. Finally, 4% BAS possessing a high thermal conductivity than 2% BAS may have also led to a higher evaporation rate. Nevertheless, it was revealed that biochar amendment resulted in controlled evaporation rates.

3.8 Effect of biochar content on crack intensity of slurry specimens under constant desiccation

Figure 15a and b display the crack intensity factors (CIF) [34] and crack reduction percentages (CRP) [39] calculated for all slurry specimens using Eq. (6) and Eq. (7), respectively. Since all slurries were prepared at the same moisture content, the initial moisture content is believed to have had a minimal effect on the cracking behaviour observed for all specimens.

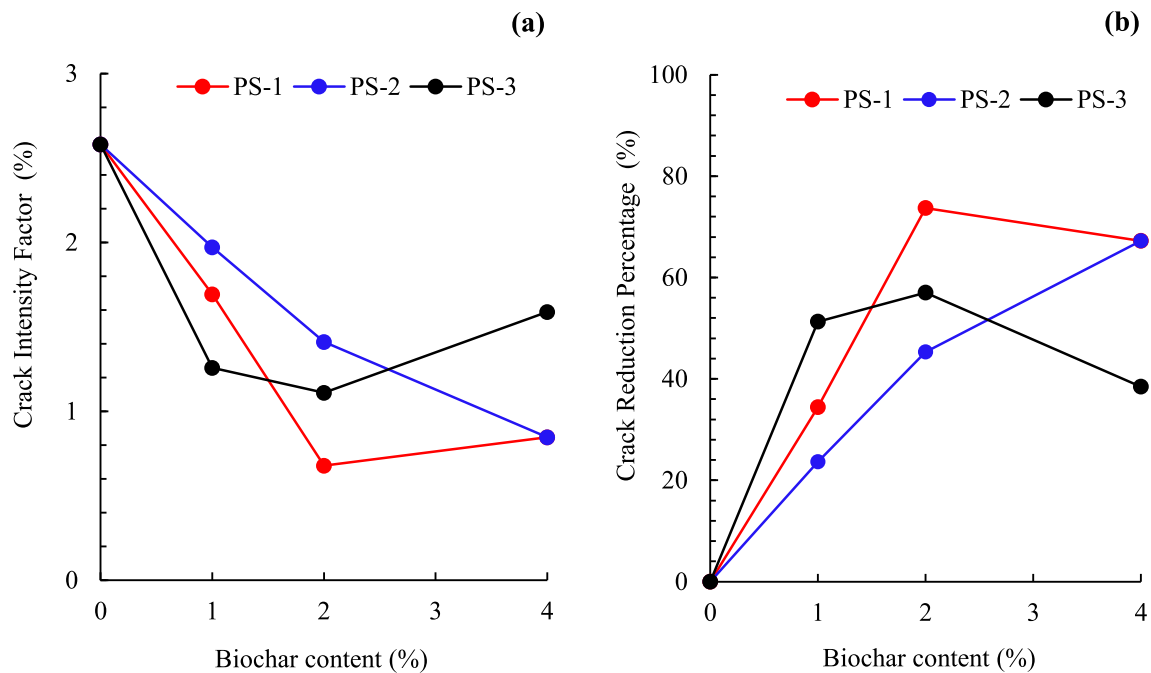


Fig. 15 Crack behaviour of slurry specimens with varying biochar content and particle size: **a** crack intensity factor (CIF); **b** crack reduction percentage (CRP)

$$\text{Crack Intensity Factor (\%)} = \frac{A_C}{A_T} \times 100 \quad (6)$$

$$\text{Crack Reduction Percentage (\%)} = \frac{CIF_{NS} - CIF_{BAS}}{CIF_{NS}} \times 100 \quad (7)$$

The terms, A_C , A_T , CIF_{NS} and CIF_{BAS} refer to total crack area of specimen, total surface area of specimen, CIF of natural soil and CIF of the related BAS specimen, respectively. The CIF value quantitatively describes the percentage of specimen area that has cracked, whereas the CRP value of a specimen indicates the relative reduction in cracking achieved by that specimen with respect to the cracking extent observed for the natural soil. Figure 15a shows that for all biochar contents (irrespective of the particle size), the CIF decreased significantly compared to natural soil. Figure 15a shows that PS-1, PS-2 and PS-3 categories of biochar achieved maximum CIF reductions of approximately 73%, 67% and 57%. For both PS-1 and PS-3 particle size categories, the cracking reduced with increasing biochar percentage up to a content of 2% content, and then, at 4% content, the CIFs calculated were higher than that of 2% BAS. However, at 4% BAS, PS-1 and PS-3 still achieved 67% and 38% CIF reductions, respectively. Alternatively, the pattern noticed for PS-2 was quite different. For PS-2, the CIF was observed to decline steadily until the 4% content itself. Hence the maximum CIF reductions for the tested specimens were

achieved at 2%, 4% and 2% biochar contents for PS-1, PS-2 and PS-3, respectively.

Researchers in the past have given numerous explanations as to why biochar addition would reduce cracking behaviour of the amended soil. One obvious explanation is that due to its random distribution, biochar (which is a non-plastic material with a high particle strength) would have occupied the shrinkage spaces of soil and reduced contraction of the soil, which would have led to limited cracking [65]. Another explanation would be that due to the increased number of micropores generated by biochar incorporation and the presence of hydrophilic functional groups in biochar particles, the BAS specimens would have been able to retain a higher volume of water compared to the natural soil during drying. The narrow micropores would have been able to hold water tightly within, owing to the functional group effect and forces that would have arisen from the capillary effect. Consequently, the volume of moisture lost during evaporation would have reduced and helped keep the BAS specimens relatively hydrated during the drying period, compared to natural soil [20, 25].

More specifically, the retention of a high volume of water within the BAS matrix would have aided in reducing the CIF via two methods: (1) increased retention of water within pores would have led to reduced matric suction in pores which would have in turn reduced the magnitude of tensile stresses that developed within the BAS matrix; (2) high volume of water would have led to the presence of more hydrogen bonds and van der Waals' forces which

would have resisted crack development [20, 24]. Alternatively, the carbon particles introduced by biochar incorporation would have functioned as organic cores around which clay, silt particles and aggregates bound via chemical, physical and biological forces which led to soil aggregation (i.e. formation of soil microaggregates and macroaggregates) and flocculation. Consequently, the improved aggregate stability by biochar would have resisted the deformation caused by external forces related to water (such as shrinkage forces caused due to drying) [9]. Moreover, the inherently low thermal conductivity of biochar would have also led to reduced evaporation via the limitation of heat flow that would have reached water molecules stored within pores and led to water loss [31].

However, while low contents of biochar aid in the reduction of drying-induced shrinkage and matric suction, its impact on desiccation cracking is known to be negative when applied at higher contents such as 4%. Accordingly, Fig. 15a and b show that the cracking areas for both PS-1 and PS-3 categories suddenly increased at 4% biochar content. This could be attributed to the tensile strength reduction of BAS caused by biochar incorporation at large application rates [9, 67]. The “tensile strength” of a soil plays a major role in resisting the tensile stresses that develop within the soil matrix due to drying-induced matric suction and shrinkage effects. Once the developed tensile stresses exceed the tensile strength of soil, the stresses will be released via cracking. Blanco-Canqui [9] attributed tensile strength reduction of the BAS to the weakening of inter-particle bonds and cohesiveness that existed between soil particles with the inclusion of excessive amounts of biochar. While soil particles binding around carbon particles would have resulted in soil aggregation, flocculation and improved aggregate stability, the excessive soil aggregation caused by inclusion of a high biochar content would have led to reduced contact between the mineral particles themselves [32, 63]. Zong et al. [67] stated that the carbon particles reduced mineral–mineral particle contacts and kept the soil mineral surfaces from bonding together which declined the cohesiveness of the soil. Zaffar et al. [63] mentioned that when used in excessive contents, the inherent porosity of biochar particles and their replacement of soil particles would reduce the contacts between the soil particles. Lu et al. [32] reported the possibility of biochar particles weakening the inter-particle bonding strength between soil clods and hence tensile strength of the soil, via a lubrication effect. Moreover, a high volume of biochar would have led to a high volume of water retention, which might have softened the cohesive bonds between clay particles due to the thick moisture layers that would have formed around clay particles [63]. Alternatively, tensile strength reduction of BAS may have also been caused due to the fact that biochar possessed a

higher number of failure planes, more microcracks and weaker contact points compared to mineral phases [68].

Interestingly however, the negative effects of biochar at 4% content were not observed for the PS-2 particle size. Therefore, it is inferred that the degree to which a soil experiences negative effects at a high biochar content is controlled by the particle size of that incorporated biochar as well. Nevertheless, it cannot be denied that one of the key means of minimizing the desiccation cracking of marine soil lies in incorporating just the correct amount of biochar which would provide the maximum resistance against cracking of the BAS.

3.9 Effect of biochar particle size on crack behaviour of slurry specimens under constant desiccation

Besides biochar content, biochar particle size was also found to affect the cracking extent of BAS specimens. One important fact noticed was that no single biochar particle size performed best for all contents. Each content had a different particle size that achieved the maximum reduction of cracking for that specific content. Figure 15a and b shows that for 1% biochar content, the PS-3 particle size performed best, by reducing the cracking by 17% and 28% more than PS-1 and PS-2, respectively. At 2% content, it was PS-1 that achieved the minimum cracking by reducing CIF by 28% and 16% more than PS-2 and PS-3, respectively. Finally, at 4% content, both PS-1 and PS-2 achieved the highest reduction of CIF which was 29% higher than PS-3 category.

At very low contents of biochar such as 1%, the fine sized biochar particles (PS-3) was the most effective in crack minimization. Due to their extreme fine size and high external specific surface area, the PS-3 biochar particles would have been able to better fill the shrinkage spaces, retain more water via the formation of more micropores/mesopores and improve aggregate stability of the BAS via the formation of more soil aggregates by bonding with carbon particles [9, 66]. Furthermore, with reference to Fig. 5d, it could be presumed that (even at slurry state) BAS belonging to the PS-3 category would have possessed the lowest thermal conductivity due to the introduction of more (1) contact points between biochar–biochar and/or biochar–soil particles and (2) tortuous heat flow paths in the BAS matrix [22, 64]. Low thermal conductivity would have reduced the magnitude of heat that reached the water molecules within the BAS pores and minimized their evaporation. All these factors would have led to the fine PS-3 biochar particles being better able to resist cracking of the BAS matrix compared to the coarser particles at low contents. However, at mild to high biochar contents (such as at 2% and 4%), it is clearly observed that the coarse

biochar particles had a more significant effect on the reduction of desiccation cracking compared to the very fine PS-3 biochar particles. While the exact reasons behind this observation may not be apparent, the authors believe that this could have occurred due to three specific reasons.

The first reason involves the difference in intra-porosity between the coarse and fine biochar particles. Grinding of biochar particles to a fine powder may have led to the destruction of a certain amount of its intra-pores, which would have reduced its intra-porosity [20]. Conversely, coarser biochar particles would have had a higher intra-porosity. The reduced intra-porosity of the fine particles would have lowered their ability to retain more water. Moreover, the specific surface area (SSA) of a biochar particle includes both its inner and outer surface areas. The reduction of intra-porosity in fine PS-3 biochar particles would have reduced their inner surface area, which would have in turn led to weakened bonding with soil particles and less soil aggregation. At smaller contents, the positive effects of PS-3 biochar having a smaller particle size and higher external surface area compared to coarse biochar particles such as PS-1 would have overcome the (aforementioned) negative effects of its lower inter-porosity when the crack propagation of the BAS was reduced. However, as the content increased, it appears that the difference in intra-porosity between the fine particles and coarse particles signified, especially since at high biochar quantities the coarse particles would have introduced intrapores more significantly into the BAS system. Having a higher quantity of intra-pores would have allowed coarse biochar particles to retain more water and keep the BAS hydrated during drying. Moreover, having reasonable extents of both external and internal surface area would have allowed coarse biochar particles to improve soil aggregation more than fine particles [28].

Alternatively, the second reason involves reduced hydraulic conductivity by the presence of coarse biochar particles, since large biochar particles would have led to longer and more tortuous water pathways [30]. Decreased hydraulic conductivity would have hindered the water flow to the top surface of the BAS specimen and reduced evaporation. This would have aided in keeping the specimen hydrated during drying and in turn led to a reduction of cracking. The final reason entails increased vapour diffusion. According to Wang et al. [59], at high biochar contents, presence of fine biochar particles aids evaporation/moisture loss from the specimen due to increased vapour diffusion rate. The existence of a reasonable number of micropores would limit the water escape during drying, by holding water tightly within the pores due to forces that rise from capillary effect and also the functional group effect. However, at high contents of fine biochar particles, the production of micropores would be excessive

which would then actually *aid* the evaporation process by creating more capillary channels that increase water vapour diffusion rate [20, 25, 59].

Therefore, in order to control the cracking behaviour of marine soil or any soil type for that matter, it is absolutely vital that the design process take into consideration both the biochar content and its particle size in order to gain its maximum benefit when employed as an amendment. Most research works that have been conducted with regards to soil stabilization generally focus on the content or amendment rates. However, this study shows that particle size also plays a major role in controlling the behaviour of the amended soil. For instance, in the event that the quantity of biochar that could be employed is restricted to a certain content, the particle size that provides the maximum amendment benefits for that fixed content could be selected. Alternatively, in certain projects, the desired improvements required for the natural soil utilized could be achieved using a content that is lower than that assigned for biochar (thus saving material cost) by simply employing biochar with a different particle size. For example, from Fig. 15a and b, PS-2 biochar performs best at 4% content by reducing CIF by 67%. However, an even better CIF reduction of 73% could be obtained at only half the content (i.e. at 2%), by simply using PS-1 biochar. Hence, it is suggested that both particle size and content be considered as *equally* important factors when employing biochar as an amendment material for coastal soils.

3.10 Generalization of experimental results

It is important to note that the results of the present study cannot be generalized for all types of biochar-amended soils and field conditions present around the globe. Accordingly, the laboratory experimental results will only be applicable for palm biochar-amended (or natural) marine soils and SCI classified soils located in regions where elevated field temperatures of around 60 °C are experienced. It is therefore recommended that the present study's experiments be carried out for soils of different classifications, different biochar types and different field conditions in the future so that results could be generalized.

3.10.1 Limitations and uncertainties of laboratory experiments

In general, when results of experiments conducted under laboratory conditions are compared with those of experiments conducted under field conditions, a dissimilarity between results is often observed. This is because it is very difficult to simulate the spontaneous nature of large-scale field conditions by controlled small-/medium-scale laboratory conditions. For the present study in particular, the

limitations and uncertainties associated with the laboratory experiments that were conducted, are summarized as follows:

- The sizes of the compacted and slurry soil samples used for the laboratory tests were much smaller compared to their size in the field.
- During drying, samples were exposed to a constant temperature of 60 °C for a specific amount of time, which simulated daytime and minimal rainfall conditions in the field. However, the temperature experienced by soil in the field under such conditions will not always be constant, but instead, be subjected to variations.
- The compacted soil samples employed for the laboratory experiments were compacted at water contents that were 4% wet of optimum in order to allow for a high shrinkage while still remaining within the acceptable compaction zone (as a conservative approach). However, in the field, the compaction degree of the soil may differ based on the compaction effort applied and field conditions.
- For the thermal cycle experiments, samples were wetted for 15 h and dried for 7 h in order to simulate night-time and daytime conditions in the field, respectively. However, these estimated daytime and night-time durations may not always remain constant in the field and may often vary.

4 Conclusions

The present study mainly investigated into the effects of incorporating palm biochar (of varying particle size and content) on the swell–shrink behaviour, cracking and evaporation rates of marine soil subjected to thermal cycles and constant desiccation. Additionally, the thermal and compaction properties of the biochar-amended soils (BAS) were examined. Biochar contents of 1%, 2% and 4% were employed with particle size ranges of: (1) $600\ \mu\text{m} < \text{PS-1} \leq 2\ \text{mm}$; (2) $300\ \mu\text{m} < \text{PS-2} \leq 600\ \mu\text{m}$; (3) $\text{PS-3} \leq 75\ \mu\text{m}$. Accordingly, highlights of the main results garnered from the conducted experiments have been summarized below.

- Thermal cycle series showed that exposure of compacted PS-3 BAS specimens to thermal cycles, led to an irrecoverable reduction of the initial volume that the specimens possessed prior to being subjected any thermal cycle. This was attributed to the irreversible deformation that would have occurred within the soil–biochar fabric due to rearrangement of soil/biochar particles and destruction of pore microstructure,

following subsection to continuous wetting and drying phases. The thermal cycle series also showed that the absolute volumetric shrinkage of all specimens increased with increasing number of thermal cycles and that BAS specimens shrunk more compared to the natural soil, which was evident given the high water retention capability of BAS mixtures.

- Exposure to constant desiccation showed that both the volumetric and areal shrinkage of compacted specimens decreased with increasing PS-3 biochar content. Accordingly, 4% BAS recorded 42% and 47% as the maximum reductions in volumetric and areal shrinkage, respectively. The reduced shrinkage was attributed to high water retention capability of micropores introduced by biochar, the binding effect of biochar to form a rigid soil structure, formation of clay-C complexes and low thermal conductivity of BAS specimens.
- Under constant desiccation, compacted 2% and 4% (PS-3) BAS specimens showed lower and more controlled evaporation rates than natural soil. The controlled evaporation of BAS specimens was ascribed to the low thermal conductivity of BAS specimens, reduced permeability of the BAS matrix due to clogging of macropores by biochar particles and high water retention capability of micropores due to the functional group effect and adsorptive forces that result from capillarity.
- Exposure of slurry specimens to constant desiccation revealed that cracking effect was reduced significantly by biochar addition regardless of the biochar particle size or content. PS-1 biochar which performed the best at 2% content, recorded a whopping 73% reduction in CIF compared to natural soil. The reduction in CIF by biochar was attributed to filling of shrinkage space by non-plastic strong biochar particles, high water retention of micropores introduced by biochar particles, low inherent thermal conductivity of biochar and improvement of soil aggregate stability caused by inclusion of biochar.

Most importantly, this study discovered that the same content or the same particle size of biochar does not always offer the best results for every scenario. Hence, in practice, it is recommended that the user should know the most effective particle size and content combination of biochar that would offer the desired outcome, in order to gain the maximum benefit out of biochar as an amendment material at the lowest possible cost.

Acknowledgements The authors wish to acknowledge Monash University Malaysia for the provision of required laboratory facilities and financial support.

Funding Open Access funding enabled and organized by CAUL and its Member Institutions.

Open Access This article is licensed under a Creative Commons Attribution 4.0 International License, which permits use, sharing, adaptation, distribution and reproduction in any medium or format, as long as you give appropriate credit to the original author(s) and the source, provide a link to the Creative Commons licence, and indicate if changes were made. The images or other third party material in this article are included in the article's Creative Commons licence, unless indicated otherwise in a credit line to the material. If material is not included in the article's Creative Commons licence and your intended use is not permitted by statutory regulation or exceeds the permitted use, you will need to obtain permission directly from the copyright holder. To view a copy of this licence, visit <http://creativecommons.org/licenses/by/4.0/>.

References

1. Abu-Hamdeh NH (2003) Thermal properties of soils as affected by density and water content. *Biosyst Eng* 86(1):97–102
2. Al Zubaydi AH, Lecture A (2011) Effect of wetting and drying cycles on swell/collapse behavior and cracks of fine-grained soils. *Tikrit J Eng Sci* 18(4):71–79
3. Albrecht BA, Benson CH (2001) Effect of desiccation on compacted natural clays. *J Geotech Geoenviron Eng* 127(1):67–75
4. Aldaeef A, Rayhani MT (2015) Hydraulic performance of compacted clay liners under simulated daily thermal cycles. *J Environ Manag* 162:171–178
5. Anderson R, Rayhani MT, Rowe R (2012) Laboratory investigation of GCL hydration from clayey sand subsoil. *Geotext Geomembr* 31:31–38
6. Barnes RT, Gallagher ME, Masiello CA, Liu Z, Dugan B (2014) Biochar-induced changes in soil hydraulic conductivity and dissolved nutrient fluxes constrained by laboratory experiments. *PLoS ONE* 9(9):e108340
7. Basma AA, Al-Homoud AS, Malkawi AIH, Al-Bashabsheh MA (1996) Swelling-shrinkage behavior of natural expansive clays. *Appl Clay Sci* 11(2–4):211–227
8. Bjerrum L (1973) Geotechnical problems involved in foundations of structures in the North Sea. *Geotechnique* 23(3):319–358
9. Blanco-Canqui H (2017) Biochar and soil physical properties. *Soil Sci Soc Am J* 81(4):687–711
10. Bordoloi S, Garg A, Sreedeeep S, Lin P, Mei G (2018) Investigation of cracking and water availability of soil-biochar composite synthesized from invasive weed water hyacinth. *Biores Technol* 263:665–677
11. Costa S, Kodikara J, Barbour SL, Fredlund DG (2018) Theoretical analysis of desiccation crack spacing of a thin, long soil layer. *Acta Geotech* 13(1):39–49. <https://doi.org/10.1007/s11440-017-0602-9>
12. Cuilan W, Weida G, Whalley WR, Baoguo L (2018) Shrinkage characteristics of lime concrete black soil as affected by biochar amendment. *Pedosphere* 28(5):713–725
13. Eberemu AO (2011) Desiccation induced shrinkage of compacted tropical clay treated with rice husk ash. *International Journal of Engineering Research in Africa*. *Trans Tech Publ*, pp 45–64
14. Emmanuel E, Anggraini V, Raghunandan ME, Asadi A (2020) Utilization of marine clay as a bottom liner material in engineered landfills. *J Environ Chem Eng* 8(4):104048. <https://doi.org/10.1016/j.jece.2020.104048>
15. Emmanuel E, Anggraini V, Raghunandan ME, Asadi A, Bouazza A (2019) Improving the engineering properties of a soft marine clay with forsteritic olivine. *Eur J Environ Civil Eng* 2:1–28
16. Fröb K (2011) Measuring and modeling of soil thermal properties and ground heat flux at two different sites at Lena Delta. University of Leipzig, Siberia
17. Garg A, Bordoloi S, Ni J, Cai W, Maddibiona P, Mei G, Poulsen T, Lin P (2019) Influence of biochar addition on gas permeability in unsaturated soil. *Géotechnique Lett* 9(1):66–71
18. Günal E, Erdem H, Çelik İ (2018) Effects of three different biochars amendment on water retention of silty loam and loamy soils. *Agric Water Manag* 208:232–244
19. Hassan AA (2014) Hydraulic performance of compacted clay liners (CCLs) under simulated landfill conditions. Doctoral dissertation, Carleton University Ottawa
20. Hussain R, Bordoloi S, Garg A, Ravi K, Sreedeeep S, Sahoo L (2020) Effect of biochar type on infiltration, water retention and desiccation crack potential of a silty sand. *Biochar* 2(4):465–478
21. Hussain R, Ghosh KK, Ravi K (2021) Impact of biochar produced from hardwood of mesquite on the hydraulic and physical properties of compacted soils for potential application in engineered structures. *Geoderma* 385:114836
22. Hyunjun O (2014) Thermal resistivity dry-out curves for thirteen sandy soils. MSc thesis, University of Wisconsin-Madison
23. Kosmas C, Danalatos N, Poesen J, Van Wesemael B (1998) The effect of water vapour adsorption on soil moisture content under Mediterranean climatic conditions. *Agric Water Manag* 36(2):157–168
24. Kumar H, Cai W, Lai J, Chen P, Ganesan SP, Bordoloi S, Liu X, Wen Y, Garg A, Mei G (2020) Influence of in-house produced biochars on cracks and retained water during drying-wetting cycles: comparison between conventional plant, animal, and nano-biochars. *J Soils Sediments* 20(4):1983–1996
25. Kumar H, Huang S, Mei G, Garg A (2021) Influence of feedstock type and particle size on efficiency of biochar in improving tensile crack resistance and shear strength in lean clayey soil. *Int J Damage Mech* 30(4):646–661
26. Lehmann J, Rillig MC, Thies J, Masiello CA, Hockaday WC, Crowley D (2011) Biochar effects on soil biota—a review. *Soil Biol Biochem* 43(9):1812–1836. <https://doi.org/10.1016/j.soilbio.2011.04.022>
27. Li Y, Yang J, Jin J, Sun X, Wang L, Chen J (2014) New reversed-phase/anion-exchange/hydrophilic interaction mixed-mode stationary phase based on dendritic polymer-modified porous silica. *J Chromatogr A* 1337:133–139
28. Li Y, Zhang F, Yang M, Zhang J, Xie Y (2019) Impacts of biochar application rates and particle sizes on runoff and soil loss in small cultivated loess plots under simulated rainfall. *Sci Total Environ* 649:1403–1413
29. Licht J, Smith N, Mitchell P, Shields F (2017) Impact of lignocellulosic and hemicellulosic biochar on soil moisture in low clay soils. *J Plant Nutr Soil Sci* 180(5):576–584
30. Lim T, Spokas K, Feyerisen G, Weis R, Koskinen W (2017) Influence of biochar particle size and shape on soil hydraulic properties. *J Environ Sci Eng* 5:8–15
31. Liu Z, Xu J, Li X, Wang J (2018) Mechanisms of biochar effects on thermal properties of red soil in south China. *Geoderma* 323:41–51
32. Lu S-G, Sun F-F, Zong Y-T (2014) Effect of rice husk biochar and coal fly ash on some physical properties of expansive clayey soil (Vertisol). *Catena* 114:37–44
33. Malongweni SO, Kihara Y, Sato K, Tokunari T, Sobuda T, Mrubata K, Masunaga T (2019) Impact of agricultural waste on the shrink-swell behavior and cracking dynamics of expansive soils. *Int J Recycl Organic Waste Agric* 8(4):339–349
34. Miller CJ, Mi H, Yesiller N (1998) Experimental analysis of desiccation crack propagation in clay liners 1. *JAWRA J Am Water Resour Assoc* 34(3):677–686

35. Mishra AK, Dhawan S, Rao SM (2008) Analysis of swelling and shrinkage behavior of compacted clays. *Geotech Geol Eng* 26(3):289–298
36. Mishra PN, Zhang Y, Bhuyan MH, Scheuermann A (2020) Anisotropy in volume change behaviour of soils during shrinkage. *Acta Geotech* 15(12):3399–3414
37. Nahlawi H, Kodikara JK (2006) Laboratory experiments on desiccation cracking of thin soil layers. *Geotech Geol Eng* 24(6):1641–1664
38. Ni J, Chen X, Ng CWW, Guo H (2018) Effects of biochar on water retention and matric suction of vegetated soil. *Géotechnique Lett* 8(2):124–129
39. Olgun M (2013) Effects of polypropylene fiber inclusion on the strength and volume change characteristics of cement-fly ash stabilized clay soil. *Geosynth Int* 20(4):263–275
40. Omran SE, Shorafa M, Zolfaghari AA, Toolarood AAS (2020) The effect of biochar on severity of soil water repellency of crude oil-contaminated soil. *Environ Sci Pollut Res* 27(6):6022–6032
41. Osinubi KJ, Eberemu AO (2010) Desiccation induced shrinkage of compacted lateritic soil treated with blast furnace slag. *Geotech Geol Eng* 28(5):537–547
42. Osinubi KJ, Nwaiwu CM (2008) Desiccation-induced shrinkage in compacted lateritic soils. *Geotech Geol Eng* 26(5):603–611
43. Ouellette RJ, Rawn JD (2015) *Principles of organic chemistry*. Academic Press, London
44. Peron H, Hueckel T, Laloui L, Hu L (2009) Fundamentals of desiccation cracking of fine-grained soils: experimental characterisation and mechanisms identification. *Can Geotech J* 46(10):1177–1201
45. Philip L, Shimell H, Hewitt P, Ellard H (2002) A field-based test cell examining clay desiccation in landfill liners. *Q J Eng GeolHydrogeol* 35(4):345–354
46. Rowe RK (1998) Geosynthetics and the minimization of contaminant migration through barrier systems beneath solid waste. *Science* 2:11047
47. Sanchez M, Atique A, Kim S, Romero E, Zielinski M (2013) Exploring desiccation cracks in soils using a 2D profile laser device. *Acta Geotech* 8(6):583–596
48. Sarabadani H (2013) Hydration and shrinkage of geosynthetic clay liners under simulated landfill conditions. Carleton University, Carleton
49. Shahsavani S, Vakili AH, Mokhberi M (2020) The effect of wetting and drying cycles on the swelling-shrinkage behavior of the expansive soils improved by nanosilica and industrial waste. *Bull Eng Geol Env* 79:4765–4781
50. Shenal Jayawardane V, Anggraini V, Emmanuel E, Yong LL, Mirzababaei M (2020) Expansive and compressibility behavior of lime stabilized fiber-reinforced marine clay. *J Mater Civ Eng* 32(11):04020328
51. Sridharan A, Allam MM (1982) Volume change behavior of desiccated soils. *J Geotech Eng Div* 108(8):1057–1071
52. Sridharan A, Sivapullaiah PV (2005) Mini compaction test apparatus for fine grained soils. *Geotech Test J* 28(3):240–246
53. Tang C-S, Shi B, Liu C, Gao L, Inyang HI (2011) Experimental investigation of the desiccation cracking behavior of soil layers during drying. *J Mater Civ Eng* 23(6):873–878
54. Tay Y, Stewart D, Cousens T (2001) Shrinkage and desiccation cracking in bentonite–sand landfill liners. *Eng Geol* 60(1–4):263–274
55. Thiel R, Giroud J, Erickson R, Criley K, Bryk J (2006) Laboratory measurements of GCL shrinkage under cyclic changes in temperature and hydration conditions. In: 8th International Conference on Geosynthetics, pp 21–44
56. Trabelsi H, Hadrich B, Guiras H (2018) Evaporation, shrinkage and intrinsic permeability of unsaturated clayey soil: analytical modelling versus experimental data. *Arab J Geosci* 11(8):1–14
57. Villagra-Mendoza K (2019) Effect of biochar amended soils on infiltration processes. Technische Universität Hamburg
58. Wang H, Garg A, Huang S, Mei G (2020) Mechanism of compacted biochar-amended expansive clay subjected to drying–wetting cycles: simultaneous investigation of hydraulic and mechanical properties. *Acta Geophys* 68(3):737–749
59. Wang T, Stewart CE, Sun C, Wang Y, Zheng J (2018) Effects of biochar addition on evaporation in the five typical Loess Plateau soils. *Catena* 162:29–39
60. Yang B, Xu K, Zhang Z (2020) Mitigating evaporation and desiccation cracks in soil with the sustainable material biochar. *Soil Sci Soc Am J* 84(2):461–471
61. Ye H, Chu C, Xu L, Guo K, Li D (2018) Experimental studies on drying-wetting cycle characteristics of expansive soils improved by industrial wastes. *Adv Civil Eng* 2:1147
62. Yesiller N, Miller C, Inci G, Yaldo K (2000) Desiccation and cracking behavior of three compacted landfill liner soils. *Eng Geol* 57(1–2):105–121
63. Zaffar M, Jamil M, Abassi G, Nafees M, Rafey M, Kamran M (2017) Biochar and fly ash role in improving mechanical and physical properties of vertiso I. *Sarhad J Agric* 33(1):151–161
64. Zhang N, Yu X, Pradhan A, Puppala AJ (2015) Effects of particle size and fines content on thermal conductivity of quartz sands. *Transp Res Rec* 2510(1):36–43
65. Zhang Y, Gu K, Li J, Tang C, Shen Z, Shi B (2020) Effect of biochar on desiccation cracking characteristics of clayey soils. *Geoderma* 364:114182
66. Zhang Y, Gu K, Tang C, Shen Z, Narala GR, Shi B (2020) Effects of biochar on the compression and swelling characteristics of clayey soils. *Int J Geosynth Ground Eng* 6:1–8
67. Zong Y, Chen D, Lu S (2014) Impact of biochars on swell–shrinkage behavior, mechanical strength, and surface cracking of clayey soil. *J Plant Nutr Soil Sci* 177(6):920–926
68. Zong Y, Xiao Q, Lu S (2016) Acidity, water retention, and mechanical physical quality of a strongly acidic Ultisol amended with biochars derived from different feedstocks. *J Soils Sediments* 16(1):177–190

Publisher's Note Springer Nature remains neutral with regard to jurisdictional claims in published maps and institutional affiliations.